



12-2008

Characterization of the Metallothionein cDNA *AgMt84* and *Pteris vittata* Tissue Culture for Phytoremediation

Blake Lee Joyce
University of Tennessee - Knoxville

Follow this and additional works at: https://trace.tennessee.edu/utk_gradthes

 Part of the [Plant Sciences Commons](#)

Recommended Citation

Joyce, Blake Lee, "Characterization of the Metallothionein cDNA *AgMt84* and *Pteris vittata* Tissue Culture for Phytoremediation. " Master's Thesis, University of Tennessee, 2008.
https://trace.tennessee.edu/utk_gradthes/452

This Thesis is brought to you for free and open access by the Graduate School at TRACE: Tennessee Research and Creative Exchange. It has been accepted for inclusion in Masters Theses by an authorized administrator of TRACE: Tennessee Research and Creative Exchange. For more information, please contact trace@utk.edu.

To the Graduate Council:

I am submitting herewith a thesis written by Blake Lee Joyce entitled "Characterization of the Metallothionein cDNA *AgNt84* and *Pteris vittata* Tissue Culture for Phytoremediation." I have examined the final electronic copy of this thesis for form and content and recommend that it be accepted in partial fulfillment of the requirements for the degree of Master of Science, with a major in Plant Sciences.

C. Neal Stewart, Major Professor

We have read this thesis and recommend its acceptance:

Beth Mullin, Zong-Ming Cheng, Arnold Saxton

Accepted for the Council:

Carolyn R. Hodges

Vice Provost and Dean of the Graduate School

(Original signatures are on file with official student records.)

To the Graduate Council:

I am submitting herewith a thesis written by Blake Lee Joyce entitled “Characterization of the Metallothionein cDNA *AgMt84* and *Pteris vittata* Tissue Culture for Phytoremediation.” I have examined the final electronic copy of this thesis for form and content and recommend that it be accepted in partial fulfillment of the requirements for the degree of Master of Science, with a major in Plant Science.

C. Neal Stewart, Jr.
Major Professor

We have read this thesis
and recommend its acceptance:

Beth Mullin

Zong-Ming Cheng

Arnold Saxton

Accepted for the Council:

Carolyn R. Hodges
Vice Provost and Dean of the Graduate School

(Original signatures are on file with official student records.)

Characterization of the Metallothionein cDNA
AgNt84 and *Pteris vittata* Tissue Culture for
Phytoremediation

A Thesis
Presented for the
Master of Science
Degree
The University of Tennessee, Knoxville

Blake Lee Joyce
December 2008

Acknowledgements

First, I wish to thank Neal Stewart for the support, funding, and mentoring that he has provided me. Above all, I am most thankful for his kindness and constant belief in me. Secondly, I wish to thank Beth Mullin for the seemingly infinite amount of patience and time she has spent with me throughout this project. I also want to thank my committee members Arnold Saxton and Zong-Ming Chang for all of their assistance in improving both this thesis and my understanding of the scientific process.

I owe a great debt of gratitude to all the people in the Stewart lab. I would like to specially thank Jason Abercrombie for mentoring me throughout my project. I am also very grateful to Mitra Mazarei, Murali Rao, Dave Mann, Hani Al-Ahmad, Laura Good Abercrombie, Wusheng Liu, Brian Leckie, Reginald Millwood, and Jason Burris for all of their assistance.

To all of my family and friends, I want thank you for your eternal enthusiasm, support, understanding and love. It is for you and the hope of improving your world that I originally began in the scientific field. Lastly, I want to thank Bridgid Lammers for helping to make a home for me in Knoxville, TN.

Abstract

Contamination of soils with toxic metals such as arsenic and cadmium has become a major environmental and human health risk. Phytoremediation provides a method to remove contaminants from soils that is not only economically viable but also environmentally sound. Metallothioneins are proteins that have the capability to bind divalent metal ions such as Ni^{2+} , Zn^{2+} , Co^{2+} , Cu^{2+} and Cd^{2+} . In this study, a concatemer sequence was designed to try to increase the presence of metal-binding proteins in transgenic plants. Two methods to increase translational efficiency of the metallothionein protein were used: 1) characterization of the full-length metallothionein *AgMt84* gene, and 2) construction of three vectors containing different fragments of the *AgMt84* cDNA which were transformed into *Nicotiana tabacum*. The concatemer sequence proved toxic to *Escherichia coli* cells and could not be cloned into vectors for plant transformation. Explants genetically transformed with vectors containing either the entire *AgMt84* cDNA or the 5' untranslated and coding region of the cDNA recovered from tissue culture. Explants genetically transformed with a vector containing only the coding region of the cDNA produced shoots but not roots in tissue culture, and then became necrotic. Characterization of the transformants is underway. The first exon and portion of the intron of the gene has been sequenced.

Phytosensors that can recognize and report the presence of arsenic would provide remediators with a management tool for phytoremediation. A transmission and scanning electron microscopy study of *Pteris vittata* tissue culture revealed callus formation on

epidermal cells of gametophytes, presence of an extracellular matrix on calli, and the formation of croziers during differentiation. Calli induced on semi-solid medium consisted of distinct meristematic nodules. These nodules differentiated randomly, and are unfit for genetic transformation. A new differentiation medium is also described.

A preliminary genetic transformation study was successful in creating protoplasts from both *Pteris vittata* gametophytes and sporophytes, but unsuccessful with biolistic bombardment of calli. Low yields, cellular debris, and autofluorescence exhibited by the protoplasts hampered polyethylene glycol-mediated genetic transformation and detection of transgene expression.

Table of Contents

	Page
Chapter One: Introduction	1
Remediation of contaminated soil	1
Metal toxicity	5
Metallothiostins.....	7
Hyperaccumulators, bioremediation, and heavy metals	9
The use of <i>Pteris vittata</i> for phytoremediation.....	12
Tissue culture of <i>Pteris vittata</i>	13
Possible transformation techniques.....	15
Fern genomics, transcriptomics, and proteomics.....	17
Objectives	20
Chapter Two: Assessing the Phytoremediation Potential of the Metallothiostin cDNA	
<i>AgNt84</i>	21
Introduction.....	21
Methods and Materials.....	24
cDNA constructs.....	24
<i>Agrobacterium</i> -mediated transformation of <i>Nicotiana tabacum</i>	26

Full length gene discovery	27
Results.....	28
Concatemer sequence.....	28
cDNA constructs and transformation of <i>Nicotiana tabacum</i>	29
<i>AgNt84</i> gene discovery	31
Discussion.....	34
Chapter Three: SEM and TEM Characterization of <i>Pteris vittata</i> Callus Induction and	
Regeneration	42
Introduction.....	42
Materials and Methods.....	46
Environmental conditions and tissue culture	46
Fixation	47
Results.....	48
Callus induction in lit versus dark conditions.....	48
Maintenance of callus on semi-solid and liquid medium	50
Differentiation of callus into sporophytes.....	56
Discussion.....	60
Chapter IV: A Preliminary Investigation of Techniques for Genetic Transformation of	
<i>Pteris vittata</i>	68

Introduction.....	68
Materials and Methods.....	69
Tissue culture of <i>Pteris vittata</i>	69
Protoplast isolation.....	69
Biolistic bombardment of induced callus	70
Results.....	71
Protoplasts.....	71
Biolistic bombardment.....	74
Discussion.....	76
References.....	78
Vita.....	95

List of Tables

Table 1. Primers used to amplify fragments of the metallothionein cDNA <i>AgMt84</i>	25
Table 2. Construct name, fragment of <i>AgMt84</i> cDNA present in construct, and number of cell lines recovered from genetic transformation of <i>Nicotiana tabacum</i>	30
Table 3. The ratio of <i>Pteris vittata</i> callus with differentiating sporophytes (regeneration efficiency) and average number of sporophytes per callus after one month on two media types.	59
Table 4. Tissue type, promoters and marker genes used in biolistic bombardment of <i>Pteris vittata</i> callus.	75

List of Figures

Figure 1. The designed <i>AgNt84</i> concatemer	29
Figure 2. Comparison of gradient PCR of <i>Alnus glutinosa</i> genomic DNA to a Southern blot membrane probed with <i>AgNt84</i> fragment.	32
Figure 3. Nested PCR with 1-655, 1-373, and 74-373 primers sets using extracted bands of interest as template.....	33
Figure 4. An alignment of the metallothionein cDNAs <i>AgNt84</i> and <i>AgNt164</i> to a sequence derived from the 1.2 kb band amplified using primer set <i>AgNt841F</i> and <i>AgNt84373R</i>	35
Figure 5. A diagram depicting the life cycle of ferns.. ..	44
Figure 6. Light microscopy of gametophytes and callus grown on callus induction medium under dark and lit conditions	49
Figure 7. Scanning electron microscopy of <i>Pteris vittata</i> gametophytes grown under lit conditions for six weeks and eight weeks	51
Figure 8. Scanning electron microscopy of <i>Pteris vittata</i> gametophytes grown on callus induction medium in dark conditions for six weeks and eight weeks.....	53
Figure 9. Transmission electron microscopy and scanning electron microscopy of <i>Pteris vittata</i> callus maintained on semi-solid callus induction medium in lit and dark conditions and liquid medium in dark conditions	57
Figure 10. Regenerating callus grown on differentiation medium under lit conditions for four weeks and eight weeks.....	61

Figure 11. Protoplasts isolated from *Pteris vittata* sporophytes and gametophytes 72

Figure 12. Flow chart of *Pteris vittata* protoplast isolation optimization..... 73

Figure 13. Transformation of *Nicotiana tabacum* cv. Xanthi controls with pAHC25-
gfp5er..... 74

Chapter One: Introduction

Remediation of contaminated soil

Pollution has far reaching influences and effects throughout the world. Mining practices, combustion of fossil fuels, industrialization, and types of metal production have mobilized heavy metals into the environment in concentrations that significantly exceed natural background sources (Clemens 2006). Specifically, soil contaminated with heavy metals pose a challenge for remediators charged with the task of cleaning up after mining and smelting practices.

Traditionally, excavation and storage of contaminated soil in hazardous waste landfills was the most effective, if expensive, way to deal with heavy metals. In 2000, the price for excavation and storage of a hectare soil dug 30 cm deep was estimated at \$1.6 million (Cunningham and Berti 2000). Worse yet, the end product for the high cost of excavation is simply moving the problem somewhere else rather than remediation. Other engineering strategies like soil washing uses surfactants and/or chelating agents to leach the contaminants out of soil once it has been excavated (Ehsan et al. 2006). This leachate is then stored or processed to, in theory, recover the contaminants for other uses. This system is less expensive than storage, and recovers large particulates from the contaminated soil while the finer particulates are lost. This technique, however, still requires excavation which is highly invasive and expensive.

Newer techniques such as electrokinetic remediation have been developed to replace excavation. This technique employs a direct current applied to soils through an anode and cathode. Groundwater or a processing fluid must then be injected into the soil to conduct the electrical potential in a field that attracts negatively charged compounds to the anode and positively charged species to the cathode (Acar and Alshwabkeh 1993). The species are then input into the system through the electrodes either by electrolysis or through the cycling processing fluid. Once the metal species are collected, they are extracted by precipitation, ion exchange, or electrodeposition (Acar and Alshwabkeh 1993).

But electrokinetic remediation has limitations; contaminants that are bound to soil particles, in their precipitate form, or were absorbed into the soil as an immiscible liquid cannot be effectively removed (Kaya and Yukselen 2005). Surfactants can be used to increase metal solubility and mobility during electrokinetic remediation. Kaya and Yukselen (2005) demonstrated that pH of surfactants varied slightly due to the concentration of the surfactant, the type of soil it is applied to, and what type of surfactant is used. They also noted that around neutral pH heavy metals precipitated in the surfactant making electrokinetic remediation ineffective. Over a period of three years, the total cost for electrokinetic remediation has been estimated at 50-120 United states dollar m^{-3} (Virkyute et al. 2002). To remediate a hectare of land up to a meter in depth, the cost would be \$500,000-1,200,000. The cost to implement phytoremediation has been estimated at \$279,000 per hectare (Cunningham and Berti 2000).

Phytoremediation is an alternative to engineering techniques. Phytoremediation seeks to employ low-cost plant mechanisms to remove inorganic pollution, such as heavy metals, from the soil. Phytoremediation techniques include phytostabilization, phytovolatilization, and phytoextraction. Phytostabilization uses plants to act on contaminated soil in several ways. Grass species are used to grow in thick clusters that reduce water and rain drainage and leaching of the contaminants from the soil into the water table. The root system of the plants binds the soil in place and reduces or eliminates erosion which would spread the contamination to other sites. The root system also stabilizes contaminated dust from wind dispersion. Though this technique does not remove the contaminant from the system, it would be most effectively used in heavily contaminated soils where nothing can grow except for plants that can exclude the metals from entering their roots. The species used for phytostabilization can also be tailored to local conditions reducing the concerns from invasive species introduction (Frérot et al. 2006).

Phytovolatilization has two steps: first the plant's root system extracts contaminants from the soil and then the plant reduces or breaks down the contaminant so it is volatilized through stomata. The best example of this technique comes from transformation of *Arabidopsis thaliana* with two bacterial genes that code for mercuric ion reductase, *merA*, and organomercury lyase, *merB*. The transgenic *Arabidopsis thaliana* produced Hg(0) gas and survived on medium containing methylmercury (Bizily et al. 2000). This strategy removes contaminants from the ground environment, but

introduces remediated substrate to the global environment through air currents. There are still many questions about the safety of producing gases from contaminants like heavy metals, and what levels of these kinds of gases are safe.

Phytoextraction uses plants that are capable of taking up environmental contaminants through their roots, and then sequestering them in aerial parts. The effectiveness of this process depends on several factors: the extent of soil contamination, the bioavailability of metal species present for uptake, and the plant's ability to absorb and accumulate the metal into shoots and leaves (Ernst 1996).

Bioavailability varies widely and depends on the metal and environmental conditions such as the physical, chemical, and biological composition of the soil. Metals, with the exception of mercury, must be in an aqueous solution to be bioavailable (Lasat 2002). If they are strongly bound to soil particles or are in their precipitate form, plant roots cannot absorb them. To ameliorate this situation, plant roots exude various compounds. Compounds called "phytometallophores" are metal chelating organic ligands that are exuded when the plant undergoes the stress of metal deficiency (Fan et al. 1997). These authors used barley roots to study a subclass of phytometallophores called phytosiderophores, more specifically mugineic acids, which are specialized to increase the bioavailable iron in the soil. It was observed that with increased iron deficiency, the levels of mugineic acids exuded not only increased, but also assumed a larger fraction of the exudate.

Economics are the final component of any remediation strategy. To create a functional strategy, whether engineering or phytoremediation, we must consider the initial price, the available capital, the extent of remediation sought, the timeframe, and the expected economic, environmental, and health benefit to the landowner/public. Economic analysis of remediation strategies is complicated because consideration must be given to local and national governmental heavy metal standards and policies, as well as the myriad of land use options available to the landowner, i.e. remediation, asphalt capping for a parking lot, a shift to crops that accumulate less metals from the soil.

An assessment of the economic value farmers would gain by using *Salix* trees to remove cadmium from contaminated soils concluded that the value of remediating ranged from €1800-21,100 ha⁻¹; this value, however, depended on factors such as the time needed to clean the soil, the value of that can be produced on the cleaned land, and the length of time a high value crop can be produced on the land after it has been cleaned (Lewandowski et al. 2006).

Metal toxicity

Metals cause cellular damage and death through several mechanisms. Their action in the cell ranges from free radical creation to osmotic balance complication. Free radicals such as superoxide (O₂^{·-}) and hydrogen peroxide (H₂O₂) damage DNA, proteins, and lipid membranes through oxidation. Superoxide and hydrogen peroxide are generated through reactions with metals such as iron (the Fenton reaction) and copper

(the Haber-Weiss reaction) that have unpaired electrons which they donate to reduce oxygen (Briat and Lebrun 1999). Hydroxyl radicals can cause DNA damage by adding hydrogen atoms to bases or removing hydrogen atoms from DNA backbones (Baker et al. 1994). Free amino acids and proteins that contain histidine, lysine, proline, and cysteine are targets for oxidation which can lead to degradation by proteases (Briat and Lebrun 1999).

Cadmium toxicity in plants results in inhibition of stomatal opening, lower growth, leaf chlorosis, oxidative stress, and replacement of zinc, thus interfering with Zn-dependent processes (Clemens 2006). Of these, Clemens states that replacement of zinc may be the most likely mechanism *in vivo*. Hart et al. (1998) suggests that cadmium moves across the plasma membrane of the cell by a native zinc carrier-mediated system. Clemens (2006) also states that cadmium binds to glutathione, thereby leading to lipid peroxidation through glutathione depletion. Membranes with higher amounts of polyunsaturated fats are more susceptible to lipid peroxidation by oxygen radicals and transition metals such as iron (Briat and Lebrun 1999).

Metals can also bind to the cell's nucleus and cause promutagenic events like DNA strand breaks, base modifications, rearrangements, and purination (Kasprzak 1995). Chromium and nickel are two human carcinogens which cause DNA alterations through metal-induced promutagenic oxidation (Waalkes et al. 1992), but there are other mechanisms for metal-induced DNA damage. Nickel competes with chromatin-bound magnesium ions, resulting in condensed chromatin, which is then hypermethylated and

therefore, not transcribed, thus silencing any oncogene suppressors present (Lee et al. 1995).

Metallohistins

The metallohistin cDNAs *AgNt84* (GenBank U69156) and *Ag164* were isolated from the root nodules of *Alnus glutinosa* in association with the actinomycete *Frankia spp.* (Pawlowski et al. 1997). Based on in situ hybridizations, these authors report that expression of *AgNt84* occurs in the second zone of *Alnus* nodules where some nonmeristematic cells are infected by *Frankia* filaments.

Before metallohistins were characterized, metal chelating proteins called metallothioneins and phytochelatins were classified. Metallothioneins are cysteine rich molecules that provide thiols for metal chelation when in their reduced form. They were first discovered in equine kidneys containing 20 cysteine residues amongst 61 amino acids (Rausser 1995). Metallothioneins are broken down into two classes based on structure: MT-I and MT-II. Metallothioneins and phytochelatins are rich in cysteine residues and are able to bind many different metal species, including copper and zinc (Mejare and Bulow 2001, Murphy et al. 1997).

MT-Is are the archetypal metallothioneins and have two domains; one domain contains nine cysteine residues that bind three metal ions, whereas the second domain has eleven cysteine residues that bind four metal ions (Rausser 1999). Rausser (1999) classifies MT-IIIs as metallothioneins that lack homology to MT-Is in the positioning of

their cysteine residues. MT-IIs are found in nematode, fungi, cyanobacteria, *Drosophila*, and plants.

Phytochelatins are repeated dipeptides of γ -GluCys that are not created through translation of gene-encoded mRNAs. Instead, they are created from glutathione and other related compounds by the enzyme PC synthase (Cobbett and Goldsborough 2002). They were found to be the major peptide bound to cadmium in complexes inside of fission yeast and plant cells (Rauser 1995). Rauser also reported that phytochelatins bind to cadmium and less frequently with copper. *In vitro* experiments on phytochelatins showed that they could release bound metals to enzymes that required them (Thumann et al. 1991). Other experiments showed that phytochelatins were capable of both protecting and reactivating enzymes such as Rubisco after undergoing cadmium stress (Kneer and Zenk 1992).

Metallohistins, on the other hand, are glycine and histidine rich actinorhizal nodulins that are not related to metallothioneins and phytochelatins (Gupta et al. 2002). The cDNA *AgNt84* codes for a 10.57 kDa, 99 amino acid protein. Metallohistin proteins have a high affinity for binding to specific divalent metal ions like Ni^{2+} , Zn^{2+} , Co^{2+} , Cu^{2+} and Cd^{2+} (Gupta et al. 2002). These authors demonstrated that the metallohistin proteins can bind 1.6 moles of Cd^{2+} per mole of monomeric protein; the capacity for binding ranged from 3 to 12 atoms per protein, depending on the metal, for both *AgNt84* and *Ag164*. Metallohistins are expressed in the beginning stages of *Frankia* infection. Because they bind cobalt, zinc, and nickel, these proteins could function to regulate

growth of the *Frankia* by accumulating or withholding these necessary elements (Gupta et al. 2002).

The metallothionein cDNA contains several parts: a 5' untranslated region (UTR), the coding region which contains a signal peptide followed by the metal-binding protein, and the 3' UTR. Pawlowski et al. also note that the 3' untranslated regions in the *AgNt84* cDNA could have a role in the regulation of mRNA regulation because it is predicted to form stem-loop structures. Expressing the entire coding sequence from *AgNt84* is lethal to *E. coli*, and so a mutant that had the first 16 amino acids of the leader sequence truncated was used to achieve *in vitro* expression for initial assessment of metal-binding properties (Pawlowski et al. 1997). A construct was then made by deleting the first twenty three amino acids of *AgNt84* which truncated the protein at the predicted signal peptidase cleavage site. All subsequent metal-binding experiments were done with this truncated construct, officially named tAgNt84-6 (Gupta et al. 2002).

Hyperaccumulators, bioremediation, and heavy metals

Horace G. Byers (Byers and Knight 1935) observed that *Astragalus* spp. accumulated selenium. Since this discovery, metal hyperaccumulators have been identified in other phyla as well as other genera. Hyperaccumulators have been defined as species capable of accumulating metals in concentrations of 100 fold greater than of other species; meaning concentrations of more than 10 mg kg⁻¹ Hg, 100 mg kg⁻¹ Cd, 1000

mg kg⁻¹ Co, Cr, Cu, and Pb, and 10,000 mg kg⁻¹ Zn and Ni (Lasat 2002). Many strains of bacteria like *Xanthomonas maltophyla*, *Escherichia coli*, and *Pseudomonas putida* have the ability to catalyze reactions to reduce and precipitate metal ions like Pb²⁺, Hg²⁺, Cr⁶⁺, and SeO₄⁻ (Blake et al. 1993; Shen and Wang 1995; Park et al. 1999). A strain of *Pseudomonas maltophilia* (strain O-2) isolated at a toxic waste site in Oak Ridge, Tennessee reduced and precipitated Hg²⁺, Cr⁶⁺, Se⁴⁺, Pb²⁺, Au³⁺, Cd²⁺, Te⁴⁺, or Ag⁺ out of a nutrient broth in a few days (Blake et al. 1993).

Metal tolerance in plant hyperaccumulators follows two basic strategies: exclusion and detoxification (Baker 1981). *Agrostis tenuis* exemplifies the metal exclusion strategy (Dahmani-Muller et al. 2000). When these authors characterized the levels of zinc, cadmium, lead, and copper in *A. tenuis*, the metal concentrations in the roots were significantly higher than in leaves. They suggested that metal immobilization in the root cell walls acted as a defense strategy to exclude the metals from aerial parts of the plant.

Physiological mechanisms used for hyperaccumulation are not well understood. In 1999, Persans et al. studied the genes involved in the free histidine (His) pathway of a nickel hyperaccumulator *Thlaspi goesingense*. The free histidine pathway was thought to be a shuttle through the cytoplasm for Ni to be loaded into the vacuole. Later, Krämer et al. (2000) presented evidence that 87% of the Ni not bound to the cell wall was chelated by citrate. They further explained that the tolerance model of nickel-citrate stored in the vacuole was sufficient to explain the hyperaccumulation ability of *T. goesingense*.

Though natural hyperaccumulators exist, most suffer from undesirable traits for phytoremediation such as low biomass and slow growth (Lasat 2002). Low biomass crops are undesirable because they inhibit proper management, for example smaller plants are more difficult to harvest. Slow growing plants may not be able to accumulate metals quickly enough to keep them from leaching from soils.

The use of hyperaccumulators to remediate heavy metals seems logical, but we must determine just how effective phytoextraction is for field-scale applications, i.e., time and rate expectations to reach targets considering biomass constraints. Hernández-Allica et al. (2006) used *Thlaspi caerulescens*, a species that accumulates zinc, in a study aimed at determining the effectiveness of phytoremediation. They collected heavy metal contaminated soil from two sites that were formerly zinc and lead smelters in northern Spain and conducted a microcosm study on metal uptake by *T. caerulescens*. *T. caerulescens* accumulated levels of zinc from 1.5% to 2.2% of its dry weight in both roots and shoots of the plant without showing phytotoxic symptoms. It was also noted that *T. caerulescens* seemed to have a positive effect on soil biological activity and health, putatively through increased carbon mineralization.

Recently, a field study to determine the viability of using phytoremediation in an urban canal was carried out in Warrington, England using hybrids of *Salix*, *Populus*, and *Alnus* (King et al. 2006). These authors found low survivorship (56-62%) and low biomass production (370-530 kg ha⁻¹ yr⁻¹ dry weight) after three years. These two factors influenced metal accumulation which was also low (36 g Cd ha⁻¹ and 4.8 Zn ha⁻¹)

compared to 47 g Cd ha⁻¹ and 14.5 kg Zn ha⁻¹ in *Salix viminalis* (Hammer et al. 2003). Though phytoextraction was not useful in this particular setting due to low plant survivorship and growth, the trees were planted on soil heavily contaminated by various heavy metals, including arsenic and hydrocarbons. It may be unreasonable to expect trees to grow on freshly dredged soil that is so heavily contaminated.

The use of Pteris vittata for phytoremediation

In 2001, Ma et al. described the capabilities of an arsenic hyperaccumulating fern, *Pteris vittata*. These authors report that *Pteris vittata* was capable of accumulating arsenic up to 2.3% in its above ground biomass without displaying symptoms of toxicity. Perhaps more importantly, 93% of the arsenic present in the fern was concentrated in the leaves. This make *Pteris vittata* ideal for phytoremediation as it can accumulate large amounts of toxic arsenic in above-ground fronds that are easy to harvest and process. Since this characterization, several researchers have studied *Pteris vittata* to understand the mechanisms for its unique arsenic tolerance.

Because *Pteris vittata* naturally shows great potential as a tool for phytoremediation it is a perfect target for genetic transformation. Genetic modification of *Pteris vittata* could lead to improved efficiency in arsenic uptake for use in phytoremediation and creation of arsenic phytosensors to monitor agricultural fields and contaminated sites. Fern transformation would also yield possibilities for new areas of research investigating fern physiology and developmental biology through study of

gametophytes overexpressing genes or knockout mutants in similar fashion to current liverwort research (Ishizaki et al. 2008); research investigating fern genomics and proteomics could yield new tools for molecular biology such as promoters and genes responsible for arsenic accumulation pathways that can be transferred to other organisms to confer value-adding traits for academic research and industrial applications. To our knowledge, however, there have been no reports of transient or stable transformation of any fern species to date. Creating a protocol for fern transformation requires investigation into fern tissue culture, possible transformation techniques, and knowledge of fern genomics.

Tissue culture of *Pteris vittata*

Yukio Kato studied *Pteris vittata* in tissue culture during the 1960's and 1970's. Kato primarily studied gametophyte formation under different light regimes and medium types. When spores germinated on basal medium (500 mg L⁻¹ NH₄NO₃; 200 mg L⁻¹ KH₂PO₄; 200 mg L⁻¹ MgSO₄ · 7 H₂O; 75 mg L⁻¹ CaCl₂; 10 mg L⁻¹ ferric citrate; 3 mg L⁻¹ MnSO₄; 0.5 mg L⁻¹ ZnSO₄ · 7 H₂O; 0.5 mg L⁻¹ H₃BO₃; 0.025 mg L⁻¹ CuSO₄; 0.025 mg L⁻¹ Na₂MoO₄; 0.025 mg L⁻¹ CoCl₂; 0.0005 ml H₂SO₄; and 6,000 agar) under white light they developed into normal two-dimensional gametophytes; when mannitol was added to the basal medium only one-dimensional growth, also known as filamentous growth or protonemata, was maintained (Kato 1970). In 1967, Kato noted that under blue light normal two-dimensional gametophytes formed while spores germinating in red light produced only one-dimensional gametophytes. Two-dimensional gametophytes

developed from protonemata after sucrose was added to the basal medium. Kato concluded that accumulation of sugars or other metabolites from photosynthesis were necessary for the proper development of fern gametophytes. Perhaps more interestingly, Kato also found that in the presence of sucrose and 10 mg L^{-1} (2,4-D) friable callus developed from protonemata. Cell suspension cultures have been initiated and recovered to gametophytes from *Pteris vittata* friable callus (Kato 1964). Callus induction and apospory, formation of gametophytes without production or germination of spores, from sporophytic *Pteris vittata* pinnae has also been achieved (Kwa et al. 1991).

More recently, Yang et al. (2008) described a method to induce callus formation from gametophytes on medium with half-strength Murashige-Skoog salts (Murashige and Skoog 1962), 2.0% w/v sucrose, and 0.7% agarose supplemented with 0.5 mg L^{-1} 6-benzylaminopurine (BAP) and 0.5 mg L^{-1} gibberellic acid (GA_3). *Pteris vittata* callus was able to accumulate about three fold more arsenic in suspension than *Arabidopsis thaliana*. When put into medium with 1.0 mM of arsenic, *Pteris vittata* callus accumulated about 2.5 mg kg^{-1} dry weight of callus. Yang suggested *Pteris vittata* callus could be used in phytoremediation of arsenic contaminated water. Later in the year, Zheng et al. (2008) described a method to regenerate *Pteris vittata* callus. Calli were placed onto the same medium as Yang et al. (2008), but supplemented with 1.0 mg L^{-1} GA_3 , 0.5 mg L^{-1} BAP, and 500 mg L^{-1} lactalbumin hydrolysate. As callus was produced from gametophytes, presumably it would contain a haploid number of

chromosomes, but it is not known whether the recovered sporophytes have a doubled or single haploid number of chromosomes.

Most traditional tissue culture systems in dicot and monocots use diploid explants such as seeds or leaves to produce callus and somatic embryos for transformation. There are, however, many tissue culture and transformation techniques described to produce doubled haploid plants as diverse as *Nicotiana tabacum* (Perica et al. 1998), *Oryza sativa* (Chair et al. 1996), and single haploids in poplar (Qu et al. 2007). In poplar, a haploid anther callus induction technique was characterized to produce haploid poplar trees which would be homozygous for the gene-of-interest in the first (T_0) generation (Qu et al. 2007). The haploid plants showed no phenotypic differences from diploid poplar, and two of ten transgenic lines were doubled haploid meaning that they had undergone spontaneous chromosome doubling. Chair et al. (1996) described a protocol to extract and transform protoplasts from microspores of rice, *Oryza sativa*. The transgenic events that were recovered ranged in ploidy level from $1n$ to $5n$; this was attributed to instability of ploidy level in rice protoplasts. Despite wide changes in ploidy level exhibited by recovered plants no abnormal phenotypes were reported. This suggests that the ploidy level of fern callus should not have a significant influence on transformation.

Possible transformation techniques

Three main transformation techniques have been considered: biolistic transformation, *Agrobacterium*-mediated transformation, and transfection of protoplasts. There are no published protocols for fern transformation, and so each technique should be

considered. Biolistic transformation is a viable option for *Pteris vittata* transformation because a tissue culture system has already been described. Biolistic transformation is a difficult and demanding technique in which DNA is bound to gold and projected into tissue under helium pressure. Biolistic transformation is appropriate for plants that are recalcitrant to *Agrobacterium* infection (Moeller and Wang 2008). Creating and optimizing a biolistic transformation method for a new species requires empirical investigation testing various rupture disk pressure, flying distance, osmotic treatment regimes, and explant tissue types. Even if optimized, biolistic methods can yield very low transformation efficiency, e.g., 3% in maize (Brettschneider et al. 1997).

In 1985, Deblaere et al. described a transformation system using a disarmed *Agrobacterium* as a vector to insert any genes found between transfer DNA (T-DNA) borders into plants. Since 1985, this transformation system has been used to rapidly transform monocots and dicots, and even used as a transient assay of gene function (Bendahmane et al. 2000). *Agrobacterium*-mediated transformation is attractive because there are fewer variables to optimize and is inherently more efficient. In context of possible fern transformation, a protocol to transform the liverwort *Marchantia polymorpha* has been described (Ishizaki et al. 2008). Ishizaki used *Agrobacterium tumefaciens* to infect young thalli with a construct which contains a 35S promoter driving β -glucuronidase (GUS) expression. After transformation, thalli were placed on hygromycin selection and resistant progeny were screened through histochemical GUS staining. Southern blots and blue GUS-stained thalli confirmed insertion of T-DNA by

Agrobacterium tumefaciens. If *Agrobacterium* is capable of infecting plants from bryophytes to angiosperms, then it may be possible that *Agrobacterium* could infect pteridophytes.

Protoplasts have been isolated from several fern species and tissue types, e.g. prothalli (Maeda and Ito 1981) and sporophytic fronds (Redford et al. 1987). Protoplasts are plant cells that have been digested with cellulase and pectinase to remove the cell wall. Without the cell wall, plant cells can be transfected with plasmid DNA using polyethylene glycol (PEG) transformation in the same way as animal cells. This method exhibits a straight forward approach to genetic transformation of fern cells, and could be used to screen a large amount of promoters for expression strength. Protoplast extraction requires optimization as well, and above all, healthy and fleshy tissue to extract a large number of cells. Ferns typically have waxy sporophytic leaves that do not release many cells, and gametophytes are so small it is difficult to maintain large enough cultures for extractions. Investigators have been successful in extracting a useful number of protoplasts for transfection from monocot grass species that have recalcitrant leaves such as switchgrass (Mazarei et al. 2008). Just as the other two possible transformation techniques, protoplast extraction and PEG transfection exhibits pros and cons that must be weighed.

Fern genomics, transcriptomics, and proteomics

The most common promoters used in molecular biology for overexpression have been shown to work in dicots or monocots such as cauliflower mosaic virus (35S), maize

or rice ubiquitin, or rice actin. There are no reports of expression using these, or any, promoters in ferns to date, but several dicot and monocot promoters have been shown to work in bryophytes (Holtorf 2002). Transformation of bryophytes with monocot and dicot promoters suggests that promoters in general will work in species that are not closely related phylogenetically. One spore-specific storage protein promoter, dubbed MVP, has been characterized from ostrich fern, *Matteuccia struthiopteris* (Schallau 2008). When the promoter was tested in transgenic *Arabidopsis thaliana* and *Nicotiana tabacum* driving GUS it showed seed-specific expression but was not expressed in leaves. The promoter did contain distinct conserved sequences known as an RY consensus sequence that is found throughout related fern, cycad, gymnosperm, and angiosperm seed- or spore-specific promoters. This report of phylogenetically “ancient” promoters performing the same function in angiosperms makes promoter discovery in ferns interesting. Further work in fern genomics could yield new tissue-specific or promoters for overexpression devoid of intellectual property issues that could function in a broad spectrum of plant species from pteridophytes to angiosperms.

The transcriptome from *Pteris vittata* fronds has been studied to elucidate potential cDNAs involved in arsenic-tolerance. The cDNAs were screened in a library plated on medium containing both antibiotic selection and 4.0 mM sodium arsenate (Rathinasabapathi et al. 2006). A total of five bacterial colonies grew on arsenate from the *Pteris vittata* library, and no colonies containing the blank vector were capable of growing. A 1,140 bp sequence from these colonies coded for a functional cytosolic

triosephosphate isomerase cDNA. The cTPI from *Pteris vittata* was able to increase arsenate tolerance in an *E. coli* strain that lacks arsenate reductase, but did not increase tolerance in an *E. coli* strain that lacked an *ars* operon. The bacteria expressing the fern cTPI also accumulated more arsenic and converted more into arsenite than controls, which suggests that the protein has a role in reducing arsenic.

In similar experiments, a cDNA library created from *Pteris vittata* gametophytes that were exposed to 1.0 mM arsenic was expressed in arsenic-sensitive yeast that lacked an arsenic reductase. Amongst the transformants, one colony of yeast had its arsenic-tolerance complemented. The recombinant sequence in that colony, called *PvARC2*, coded for a 134 amino acid protein that shared 47% homology with *ScARC2*, arsenate reductase from *Saccharomyces cerevisiae*, and 60% homology with *CDC25*, a phosphatase that shows arsenate reductase activity from *Arabidopsis thaliana* (Ellis et al. 2006). The arsenate reducing rate of *PvARC2* was found to be comparable to *CDC25*, but not as high as *ScARC2*. These *in vitro* results suggest that *PvARC2* is an arsenate reductase, but its role *in vivo* has not been determined and so further work must be carried out to determine whether this protein can be useful for phytoremediation purposes. Further genomic studies such as these could provide tools for researchers to increase the phytoremediation capability of other plant species through genetic transformation.

Objectives

1. Increase translational efficiency of *AgNt84* to detectable amounts in transgenic *Nicotiana tabacum* cv. *Xanthi* for characterization of potential metal-binding trait conferred by expression of the metallothionein protein *in planta*.
2. Characterize the *Pteris vittata* tissue culture system to determine its potential use in genetic transformation techniques.
3. Investigate potential genetic transformation techniques of the fern *Pteris vittata*.

Chapter Two: Assessing the Phytoremediation Potential of the Metallothionein cDNA *AgMt84*

Introduction

Mining practices, combustion of fossil fuels, industrialization, and metal production have mobilized toxic compounds containing “heavy metals” such as arsenic, cadmium, cobalt, copper, and nickel into the environment in concentrations that significantly exceed natural background sources (Clemens 2006). Phytoremediation, the removal of specific compounds from soils using plants capable of contamination uptake and storage in aboveground growth, has recently become an attractive alternative to traditional soil contaminant removal.

In 1997, a new class of metal-binding proteins called metallothioneins was discovered (Pawlowski et al. 1997). The metallothionein protein exhibits an amazing ability to bind a wide range of divalent metal ions such as Zn^{2+} , Cd^{2+} , Ni^{2+} , Co^{2+} , and Cu^{2+} (Gupta et al. 2002). The metallothionein cDNA *AgMt84* was originally isolated from mRNA in *Alnus glutinosa* root nodules (Pawlowski et al. 1997). *AgMt84* and *AgMt164*, a closely related metallothionein homolog, mRNA is expressed in root nodules only during early stages of infection by *Frankia* spp. *AgMt84* contains several regions of interest. The coding region contains a signal peptide and the metal-binding protein. The signal peptide has an 82% prediction for transport out of the cell using WoLF PSORT protein

subcellular localization prediction for plants (<http://wolfpsort.org>). The metal-binding protein coding region contains 219 base pairs that code for 74 amino acids. Two untranslated regions (UTRs) flank the coding region both upstream (5') and downstream (3'). A second cDNA called *AgNt164* showed high DNA sequence similarity to *AgNt84* and is considered part of the metallothionein gene family (Pawlowski 1997). *AgNt84* and *AgNt164* are slightly different. *AgNt164* codes for a 9.19 kDa protein whereas *AgNt84* codes for a 10.57 kDa protein. Both cDNAs were present only in nodule RNA northern blots and were not found in shoot tips, male flowers, female flowers, and developing fruits. Though the native function of the protein is currently unknown its possible use to increase the phytoremediation capability of plants is intriguing.

Transgenic *AgNt84 Nicotiana tabacum*, *Arabidopsis thaliana*, and *Brassica juncea* were generated and partially characterized (Mentewab et al. 2005). Northern blots of the *Arabidopsis thaliana* lines showed presence of *AgNt84* mRNA, but presence of the *AgNt84* protein could not be confirmed with a specialized western blot technique designed for detection of the metallothionein protein (Maillet et al. 2001). This suggests that failure to transcribe the metallothionein cDNA could explain the lack of increased metal-binding in transgenics versus wild type. Factors such as mRNA that is degraded quickly or post-transcriptional regulation cause a failure in transcription.

Previous work has excluded the first 38 base pairs from the 5' UTR and all of the 3' UTR in constructs. Pawlowski et al. (1997) predicted the 3' UTR of *AgNt84* and *AgNt164* to form extensive stem-loop structures and have an influence on the regulation

of the mRNA. In addition, mRNA 5' and 3' UTRs play a regulatory role that affect localization, translation efficiency, and mRNA stability (Chabregas et al. 2002; Gilmartin 2005; Kertész et al. 2006; Schwartz et al. 2006; Patel et al. 2006).

The 3' UTR could have an effect on stability or targeting of the metallohistin mRNA. Schwartz et al. (2006) reported a decrease in relative mRNA abundance as the length of the 3' UTR increased in *Nicotiana benthamiana*. These authors report approximately 45% mRNA abundance from constructs with a 3' UTR of 300 bp relative to their standard gene which had a 40 bp 3' UTR. Kertész et al. (2006) found that plants trigger nonsense-mediated decay of mRNAs when the 3' UTR of the mRNA is unusually long. In a study of RUBISCO expression in C₄ plants, Patel et al. (2006) found both the 5' and the 3' UTRs were needed to have specific RUBISCO-GFP expression in basal cells. This suggests that interactions between these two regions are needed to target a protein to the correct place.

The importance of introns in post-transcriptional regulation has been the focus of recent research. Unlike most receptors, a human neuropeptide receptor Y1 (hY1) has a 97 bp intron in its coding sequence. Expression of cDNAs without the native intron IV shows low amounts of transcript, but when constructs containing intron IV either before the coding region or in its native position in the coding region significantly increased production of functional hY1 protein (Marklund et al. 2002).

This work seeks to assess potential methods to increase expression of *AgNr84* to measurable amounts in transgenic *Nicotiana tabacum* cv. *Xanthi*. Once measurable

amounts of AgNt84 protein are created in transgenic plants, researchers can gain insight into the role of the metallothionein gene *in planta* and the potential to confer metal-binding traits by expression of the metallothionein protein.

Methods and Materials

cDNA constructs

Portions of the cDNA *AgNt84* were PCR amplified with primer sets (Table 1) using pAgNt84 (Pawlowski et al. 1997) as a template under the following PCR conditions: 94 °C for 1 minute; a denaturation step at 94 °C for 30 seconds, an annealing step at 46 °C for 30 seconds, and an elongation step at 72 °C for 2 minutes repeated 35 times; a final elongation at 72 °C for 5 minutes.

The amplified fragments were separated by size using gel electrophoresis on a 1.0% agarose gel and then extracted from the gel using the QIAquick gel extraction kit (Qiagen). Extracted fragments were TOPO cloned into the vector pCR8/GW/TOPO (Invitrogen). Heat shock competent *E. coli* were transformed by adding 3 µl of the TOPO cloning reaction to 100 µl of frozen *E. coli* stocks. The plasmid-bacteria mixture was left to sit on ice for 10 minutes before placing in a 42 °C water bath for 30 seconds. The bacteria were immediately moved to 1 µl of SOB medium (2.0% w/v tryptone, 0.5% yeast extract, 0.058% NaCl, 0.0186% KCl, pH to 7.00) and left in a 37 °C incubated shaker rotating at 150 rpm. After an hour the mixture of bacteria were plated onto semi-

Table 1. Primers used to amplify fragments of the metallohistin cDNA *AgNt84*.

Primer	cDNA BP	Sequence
AgNt84-1 forward	1-23	5' – AATTAATCATCTTAGAGTTTGT – 3'
AgNt84-74 forward	74-92	5' – ATGGGTTACTCCAAGACTT – 3'
AgNt84-373 reverse	354-373	5' – CTAATTTTGGTTGGTTTCAG – 3'
AgNt84-655 reverse	631-655	5' – AGAATTCATAAACTATATATTCATC – 3'

solid LB medium (1.0% w/v tryptone, 0.5% yeast extract, 1.0% NaCl, 1.5% Bactoagar, pH to 7.00) with spectinomycin selection. Plates were placed in a 37 °C oven overnight.

Single colonies that formed overnight were restreaked and left to grow overnight once more. Surviving colonies were inoculated in test tubes containing 5 ml of liquid LB and spectinomycin selection and left to grow overnight in a 37 °C shaking incubator. Each test tube was spun down and plasmid was extracted using alkaline lysis.

After extracting plasmid DNA, each vector was digested with either PvuI or PstI to confirm their orientation in the pCR8/GW plasmid. Constructs that had the correct orientation were sequence confirmed to ensure that no mutations occurred during cloning. The pCR8 vectors containing the sequence-confirmed *AgNt84* cDNA fragments were inserted into pMDC32 (Curtis and Grossnilaus 2003) by a Gateway LR reaction (Invitrogen). The LR reaction mixture was transformed into *E. coli* and plated onto LB medium plates with kanamycin selection. Colonies were restreaked and grown in liquid medium as before. Extracted plasmids were once more digested with *HindIII* and *PstI* to confirm presence of the correct insert.

Agrobacterium*-mediated transformation of *Nicotiana tabacum

After confirmation, extracted pMDC32-*AgNr84* plasmids were used to heat-shock transform *Agrobacterium tumefaciens* EHA105. *Agrobacterium tumefaciens* EHA105 cells were grown in liquid YEP medium (1.0% w/v peptone, 1.0% yeast extract, 0.5% NaCl) until an optical density (OD) of 0.5. The bacteria cultures were then spun down at 3000 rpm on a benchtop centrifuge for 5 minutes at 4 °C. The cell pellet was resuspended in 1 ml of cold 20 mM CaCl₂ and 100 µl aliquoted into 1.5 ml tubes. Aliquots were then flash frozen in liquid nitrogen and stored at -80 °C until needed.

Heat-shock competent cells were then removed from the -80 °C freezer and 1 µg of plasmid DNA was added to the frozen pellets. Then the tubes of bacteria and plasmid DNA were moved to a 37 °C waterbath for 5 minutes. Tubes were quickly removed and 1 ml YEP medium was added to each tube. Tubes were left to shake horizontally in 28 °C incubated shakers at 150 rpm for four hours before 250 µl of the bacterial suspension was plated on semi-solid YEP plates with 50 mg L⁻¹ kanamycin. Plates were moved to a 28 °C oven for 48 hours.

Single colonies surviving selection were restreaked and then grown in 5 ml of liquid YEP medium with selection for plasmid extractions. *Agrobacterium* colonies from single colonies were scraped from semi-solid plates and boiled in distilled water for 10 minutes. The resulting suspension was spun on a benchtop centrifuge at 14000 rpm for 10 minutes. The supernatant from each tube was used for colony PCR confirmation of inserted plasmid for each *Agrobacterium* cell line that survived selection. Positive cells

were selected and grown in 5 ml liquid YEP medium with selection for transformation.

Nicotiana tabacum cv. *Xanthi* seeds were surface sterilized in 20% ethanol and 10% dilution of sodium hypochlorite (5.25% sodium hypochlorite, Fischer Scientific) and plated on semi-solid MSO (MS basal medium (Murashige and Skoog 1962) B5 vitamins (Gamborg 1968) with 3.0% sucrose, 0.2% Gelrite Gellan Gum, pH to 5.8) six weeks prior to transformation. On the day of the genetic transformation, the appropriate *Agrobacterium tumefaciens* cultures were spun down for 5 minutes at 5000 rpm and resuspended in 2.5 ml liquid DBI medium. *Nicotiana tabacum* leaf explants were cut and placed into the resuspended bacteria in a sterile Petri dish for 30 minutes. Afterwards, the explants were moved to semi-solid MSO for 2 days to co-cultivate. Then the explants were moved to semi-solid DBI with 50 μ M hygromycin and 400 μ M timentin. Explants were subcultured every two weeks until shoots formed.

Shoots were moved to semi-solid MSO with appropriate selection for rooting. Once rooted, plants were moved to soil to harden off. After one month in a controlled environment with 28°C with 16 hrs of light and 8 hours of dark plants were moved to the greenhouse. T₁ seed were collected after set, labeled, and sterilized as before and plated on MSO with 50 μ M hygromycin for selection.

Full length gene discovery

To elucidate the full length *AgNr84* gene, *Alnus glutinosa* genomic DNA was amplified with primers used in construction of the cDNA plasmids (Table 1) in 50 μ l volume reactions under the following gradient PCR conditions: 94 °C for 1 minute; a

denaturation step at 94 °C for 30 seconds, an annealing step at 50 ± 10 °C for 2 minutes, and an elongation step at 72 °C for 3 minutes repeated 35 times; a final elongation at 72 °C for 5 minutes. Gel electrophoresis of the PCR products on a 1.0% agarose gel for 1 hour at 80 volts gave sufficient separation. A picture of the gel was taken under UV light before blotting.

Nested PCR reactions were performed on extracted bands of interest using the same primer sets as above, and under the same PCR conditions. ClustalX2.09 (Larkin et al. 2007) was used to align sequenced bands of interest to *AgNt84* and *AgNt164*. Splice site prediction was performed using the NetPlantGene server (Center for Biological Sequence Analysis, <http://www.cbs.dtu.dk/services/NetPGene/>).

Results

Concatemer sequence

A concatemer sequence was designed based on the metallohistin cDNA *AgNt84*. The concatemer sequence contained the signal peptide followed by three repeats of the metal-binding protein without a stop codon (Figure 1). The final repeat of the metallohistin coding region contained the stop codon. The concatemer sequence was constructed by Blue Heron Biotechnology (www.blueheronbio.com). However, during cloning the concatemer sequence exhibited toxicity in *Escherichia coli* EC100. To avoid toxicity, the concatemer had to be created in three pieces and ligated together. When the

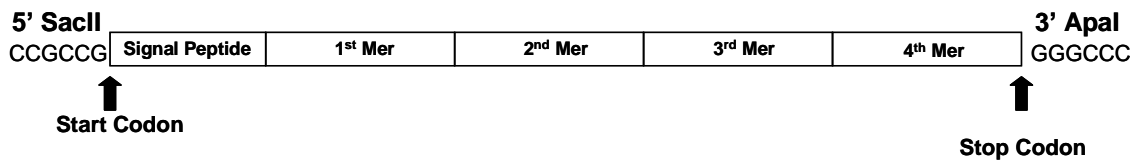


Figure 1. The designed *AgNt84* concatemer. The concatemer consists of the native signal peptide and four repeats of the coding region for the metal-binding protein ending in a stop codon.

final concatemer sequence was created and put into pUC, it was transformed into *E. coli* EC100. Only colonies containing mutations in the concatemer sequence were able to grow. Use of the stable *E. coli* cell line Stb14, the low copy vector pBR322, and growing the colonies at room temperature did not allow colonies to grow without mutations. Because the concatemer construct could not be replicated, only a polymerase chain reaction (PCR) product could be synthesized and created.

cDNA constructs and transformation of *Nicotiana tabacum*

Three constructs were created to assess whether the untranslated regions of the cDNA could have a role in *AgNt84* mRNA stability. Three cDNA fragments were PCR amplified and inserted into pMDC32: 1) the entire cDNA (1-655 base pairs); 2) the 5' UTR and coding region (1-373 base pairs); 3) the coding region only (74-373 base pairs). *Agrobacterium tumefaciens* EHA105 was used to transform *Nicotiana tabacum* cv. *Xanthi*. *Xanthi* explants transformed with pMDC32-*AgNt84*-1-655 and pMDC32-*AgNt84*-1-373 recovered shoots and roots while on hygromycin selection (Table 2). Interestingly, explants transformed with pMDC32-*AgNt8*-74-373 produced shoots on

Table 2. Construct name, fragment of *AgNi84* cDNA present in construct, and number of cell lines recovered from genetic transformation of *Nicotiana tabacum*.

Construct	Portion of cDNA	Transgenic Plant Lines Recovered
pMDC32- <i>AgNi84</i> -1-655	5' UTR, coding region, 3' UTR	17
pMDC32- <i>AgNi84</i> -1-373	5' UTR and coding region	16
pMDC32- <i>AgNi84</i> -74-373	Coding region only	0

DBI medium with hygromycin selection, but did not root when transferred to MSO medium with hygromycin. After two weeks, the shoots grew necrotic and died.

***AgNt84* gene discovery**

Alnus glutinosa genomic DNA was used as a template to amplify potential candidates for the full length *AgNt84* gene. Multiple gene products were visible for each primer set and temperature gradient (Figure 2). In order to screen the possible bands, the gel was Southern blotted onto a nitrocellulose membrane, and probed with an *AgNt84* fragment tagged with a fluorescent marker. Most of the bands present in the Southern blot match up to the brighter bands seen in the original agarose gel, but the 1.4 kb band from primer set 1-655 did not.

Seven bands were selected for gel extraction and Nested PCR analysis: 1) 3.0 kb band from 1-655 primer set; 2) 1.4 kb band from 1-655 primer set; 3) 3.0 kb band from 1-373 primer set; 4) 2.6 kb band from 1-373 primer set; 5) 1.2 kb band from 1-373 primer set; 6) 1.2 kb band(s) from 74-373 primer set; 7) 0.75 kb band from 74-373 primer set (Figure 3). Bands 1 and 2 extracted from the 1-655 primer set only amplified using the 74-373 primer set; two product bands resulted at 750 bp and 300 bp. Bands 3, 4, and 5 extracted from the 1-373 primer set amplified their proper lengths when amplified with the 1-373 and the 74-373 primer set. Multiple minor product bands were produced in bands 3, 4, and 5 when amplified with the 1-373 primer set. Band 6 and 7 extracted from the 74-373 primer set amplified their proper length with the 74-373 primer, and amplified

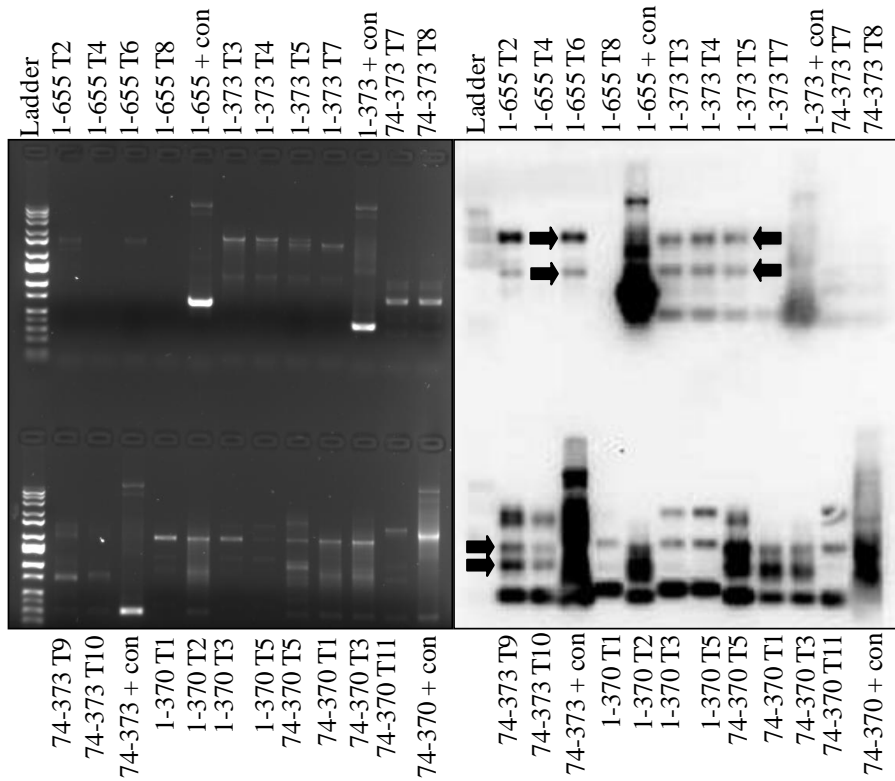


Figure 2. Comparison of gradient PCR of *Alnus glutinosa* genomic DNA to a Southern blot membrane probed with *AgNt84* fragment. Left) Gradient PCR agarose gel using selected primers specific to the *AgNt84* cDNA with *Alnus glutinosa* genomic DNA template. Right) Gel from left blotted onto a nitrocellulose membrane and probed using 33-469 bp *AgNt84* fragment. Arrows indicate bands that were chosen for nested PCR reactions. Hi-Lo DNA ladder (Bionexus, Inc) was used to mark fragment size. Note that not all of the bands from the Southern blot match to bands visible in the PCR gel.

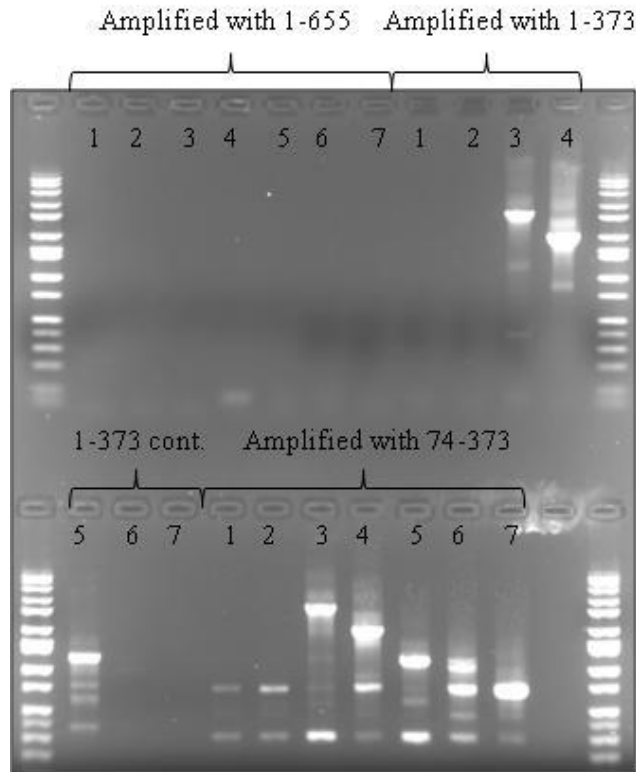


Figure 3. Nested PCR with 1-655, 1-373, and 74-373 primers sets using extracted bands of interest as template. Extracted bands were as follows: 1) 3.0 kb band from 1-655 primer set; 2) 1.4 kb band from 1-655 primer set; 3) 3.0 kb band from 1-373 primer set; 4) 2.6 kb band from 1-373 primer set; 5) 1.2 kb band from 1-373 primer set; 6) 1.2 kb band(s) from primer set 74-373; 7) 0.75 kb band from 74-373 primer set. Bands 1 and 2 extracted from the 1-655 primer set only amplified using the 74-373 primer set. Bands 3, 4, and 5 extracted from the 1-373 primer set amplified their proper lengths when amplified with the 1-373 and the 74-373 primer set. Band 6 and 7 extracted from the 74-373 primer set also amplified their proper length with the 74-373 primer, and amplified multiple other fragments. Hi-Lo DNA ladder (Bionexus, Inc) was used to mark fragment size.

multiple other fragments. Band 6 yielded a 1.2 kb, a 750 bp, and a 300 bp band when amplified with the 74-373 primer set. Band 7 only yielded a 750 bp and a 300 bp band when amplified with the 74-373 primer set. All seven extracted bands yielded a 300 bp band and most yielded a 750 bp band when amplified with the 74-373 primer set.

Closer inspection after sequencing revealed the presence of two bands, not one, at 1.2 kb length from the 74-373 primer set. This doublet mirrors the bands seen at 3.0 kb in the 1-373 primer set. All seven bands of interest were sequenced. Only the sequence derived from the 1.2 kb band from primer set 1-373 using the primer *AgNt84-1* forward matched to *AgNt84* and *AgNt164* with a high degree of homology (Figure 4). The sequence from 2-137 bp of the genomic DNA (gDNA) band aligned to the 5' end of the cDNAs from 42-179 bp of *AgNt84* and 42-150 bp of *AgNt164*. At some bases the gDNA matches to only *AgNt84* or *AgNt164* highlighted in Figure 4 in either blue or green, respectively. The homology ends at a GT base sequence in the gDNA and from 138-669 bp does not match to either cDNA again. No introns could be predicted at this site. Clean sequencing results could not be obtained using the *AgNt84-373* reverse primer from this sequence.

Discussion

Toxicity that the 4x *AgNt84* concatemer sequence exhibited in *E. coli* prevented cloning and transformation of *Nicotiana tabacum* cv. *Xanthi* from the lack of a completed vector DNA. The *AgNt84* cDNA showed toxicity in *E. coli* when large amounts of

Figure 4. An alignment of the metallohistin cDNAs AgNt84 and AgNt164 to a sequence derived from the 1.2 kb band amplified using primer set AgNt841F and AgNt84373R. Stars indicate an exact match between all three sequences. Areas highlighted in yellow are the coding region of the cDNAs. Areas highlighted in blue are bases of the gDNA sequence that match to AgNt84 but not AgNt164. Areas highlighted in green are bases of the gDNA sequence that match to AgNt164 but not AgNt84. Black arrows indicate forward and reverse primers designed specific to AgNt84 to amplify the entire putative intron. Red arrows indicate forward and reverse primers designed specific AgNt84 to amplify the remaining portion of gDNA exons and potential introns.


```

AgNt.84cDNA 1 AATTAATCATCTTAGAGTTTGTTCCTAGCTAGTACTAGTCTCCAATCCTCTTCA
AgNt.164cDNA 1 -----CCTACTACAAATTTGCTCCAATCCTCTTCA
gDNA 1 -----WTTGTTCTCCATCCTCTTC-
***** * *****

AgNt.84cDNA 61 TTGTTAACGAAAATGGGTTACTCAAGACTTTCTTCTCCTGGCCTTGGCTTTGCTGT
AgNt.164cDNA 32 TTGTTAACGAAAATGGGTTACTCAACACTTTCTCCTGGCCTAGCTTTGGCCGT
gDNA 20 TTGTTGACGAAA-ATGGGTTACTCAAGACTTTCTTCTCCTGGCTAGCTTTGCTGT
***** * *****

AgNt.84cDNA 121 TGTGCTCCTCATCTCTCCGATGTTTCAGCTCTGAGCTTGTGTGCCCTCAAACCA-
AgNt.164cDNA 92 TGTGCTCCTCATCTCTCCGATGTTTCAGCTCTGAGCTTGTGTGCCCTCAAACCA-
gDNA 79 TGTGCTCCTCATCTCTCCGATGTTTCAGCTCTGAGCTTGTGTGCCCTCAAACCA
***** * *****

AgNt.84cDNA -----
AgNt.164cDNA -----
gDNA 139 TGAGTTCTTACTTTTTCTGAATTAATTAATATGCACCTTACTATCTCTCGTTTTT

AgNt.84cDNA -----
AgNt.164cDNA -----
gDNA 199 GGTAGTGATCAAGAGCCCTGTGTTCTAAATAATGTGTAATTCCTCATATAAAGTGATA

AgNt.84cDNA -----
AgNt.164cDNA -----
gDNA 259 ATATGCATCATTGGACAAGAAAAACAGACAGAGTACTTCGAAGTACATAACGACRT

AgNt.84cDNA -----
AgNt.164cDNA -----
gDNA 319 GCCTTGCATCTCTATACATCCGTTTTACAAAATAATGGAACATCATTTCTCATGTTTCA

AgNt.84cDNA -----
AgNt.164cDNA -----
gDNA 379 TAGAATTTATTTAAGCACTTTATGTTTTTGAATTCGCGCACAACTTAATTTCCAGTA

AgNt.84cDNA -----
AgNt.164cDNA -----
gDNA 439 TAATTATAGTTTACCTTAACCATGTGTCATATATTTAACTTCTCAACTGATCATTTATG

AgNt.84cDNA -----
AgNt.164cDNA -----
gDNA 499 TCCAAACTGGTGTGTATATTTGATATATGATCAATACAATATATTTAATTTTGCA

AgNt.84cDNA -----
AgNt.164cDNA -----
gDNA 519 ATTTCTTATTTTCTATCTACTTAAATTTTGGAGAAAATTAATTTTGCATGGTATAAA

AgNt.84cDNA -----
AgNt.164cDNA -----
gDNA 579 CTCAAATGATTTGAAAAGAAAGTTAAGGACAAGTAAAAAGCTTCAAGACAAGATTCTGA

AgNt.84cDNA -----
AgNt.164cDNA -----
gDNA 639 ACAGGGGATATATCTTAGCTCTTAATTAAGACATTAATGCAAACTTAACATTACC

AgNt.84cDNA 180 AGGAGAATATGCAAACCTGACGGTGTGGAGGAGGATAAGTATCATGGCCATCGTCACGTGC
AgNt.164cDNA 151 AGGAGAATATGCAAACCTGATGGTGGCGGAGGAGTCAAGTATCATGGCCATCGTCACGTGC
gDNA -----

AgNt.84cDNA 240 ATGGACATGGGCATGGACATGTACATGGGAATGGGAATGAACATGGACATGGTCATCACC
AgNt.164cDNA 211 ATGGACATGGGCATGGGAATGGACATGG-----ACACC
gDNA -----

AgNt.84cDNA 300 ACGGCCGTGGTCAACCAGGACACGGTGTGCTGCAGACGACAGAAACCGA----AACT
AgNt.164cDNA 244 ACGGCCATGGTCACTCGGACATGTTGTTGCTGCTGATGACAGACAGAACTGATCGAAATT
gDNA -----

AgNt.84cDNA 356 GAAACCAACCAAAATTAGACCAATCTTTTGAATTCGCTCTATATAT-----
AgNt.164cDNA 303 AAACCAATCAAAATTAGACGAATCCTTCGATTCGCTCTATATATATATATATATATA
gDNA -----

AgNt.84cDNA 401 -----GCTACAGTTGTACGTACGTCTAAGTGTGTC
AgNt.164cDNA 363 TATATATATATACACATATTTGACATATATGCTACAGCTATACA---TCTGAGTGTGTC
gDNA -----

AgNt.84cDNA 432 TAAGTCGTAATATGTGGCTTAATTATCTAATTAAGCTTGTATGCCAATAAECTTTATGTT
AgNt.164cDNA 419 TAAGTCGCTTATGTGGCTTAATTATCTAATTAAGCTTGTATGCCAATAAECTTTATGTT
gDNA -----

AgNt.84cDNA 492 TCTACTTTTGTCAATGTAATTTTGTCTTTTCTATGATTTCAATGTACGCTGTAGCATA
AgNt.164cDNA 479 TCTACTTTTGTCAATGTAATTTTGTCTTTTCTATGATTTCAATGTACGCTGTAGCATA
gDNA -----

AgNt.84cDNA 552 TCAAAATTAACGAATCCTTTGCTCTATATATATATATATATATATATATATATATATAT
AgNt.164cDNA 533 TCAAAATTAACGAATCCTTTGCTCTATATATATATATATATATATATATATATATATAT
gDNA -----

AgNt.84cDNA 582 -----GCAACTTTTGAAGGCTGTACGTGAATAAGATTATA
AgNt.164cDNA 593 ATATATATATATATATATATATATATATATATATATATATATATATATATATATATATAT
gDNA -----

AgNt.84cDNA 618 TTGGATGAATATATAGTTTATGAATTCT
AgNt.164cDNA 653 TTGGCTGAATAAATAGTTTATGAATTCT
gDNA -----

```

Figure 4. Continued.

protein were induced for purification (Gupta et al. 2002). *E. coli* were able to grow normally, however, when constructs that lacked the signal peptide of the *AgNt84* cDNA were used. Though it may be possible the signal peptide caused toxicity in colonies with the designed concatemer, it is unlikely because protein production should be minimal in the low expression vector pBR322 and other constructs containing the signal peptide have been cloned and replicated in *E. coli* not only in this work, but in other work as well (Mentewab et al. 2005).

Conventional wisdom holds that *E. coli* easily mutates sections of short repeats in plasmid DNA. *AgNt84* codes for a 74 amino acid protein and was repeated four times in the concatemer. Another concatemer sequence designed using thymosin alpha 1 contained six sequence repeats each only 28 amino acids long (Zhou et al. 2008). This concatemer was successfully expressed in *E. coli* without issue. In addition, a construct with 19 repeats only 15 bp long was efficiently expressed in *E. coli* to produce elastomeric polypeptides (McPherson et al. 1992). Presence of a few short repeats alone does not seem enough to cause toxicity in all but the colonies with mutations in the concatemer protein sequence. It could be possible the toxicity observed could be related to the metallohistin protein function. It is unknown what role the metallohistin protein plays in *Alnus glutinosa* nodules, but it could be involved in binding metal ions during early nodule formation as similar proteins containing signal peptides and cysteine-rich sequences are found in soybean during association in bacterial symbiosis (Sandal et al. 1987; Pawlowski et al. 1997). Toxicity in *E. coli* could be linked to the multimeric

metallohistin proteins binding and making necessary metallic compounds inside cells unavailable for metabolism at background expression levels.

Currently, the T₁ generation of transgenic plants for pMDC32-*AgNt84*-1-655 and pMDC32-*AgNt84*-1-373 are undergoing zygosity screening. Once *AgNt84* homozygotic lines are found, they can be grown and tested for presence of mRNA and metallohistin protein. Full characterization will be completed with studies of cadmium metal-binding compared to wild-type *Nicotiana tabacum* cv. *Xanthi*.

Strangely, no lines of pMDC32-*AgNt84*-74-373 could be recovered during tissue culture. It is unlikely that tissue culture conditions were responsible for the phenotype because all transformations and subcultures were performed at the same time. Further investigation into the strange phenotype exhibited in putative pMDC32-*AgNt84*-1-655 transformants will be necessary. Further transformations will be performed with this construct. If recovered shoots will not root, protein extractions and western blots will be performed to detect presence or absence of the *AgNt84* protein.

Little is known about the role of introns in translation regulation, but recently research has begun to focus the importance of introns for translation efficiency. Expression studies of histone H1 in *Xenopus* oocytes found that there was as much as a 100-fold difference between two constructs based solely due to construct configuration (Matsumoto et al. 1998). Further investigation revealed this difference in translation was due not only to the presence of an intron in the mRNA, but also to the positioning of that intron. Constructs with an intron at the 5' end of the transcript had increased translation

efficiency whereas constructs with an intron at the 3' end of the transcript had translational efficiencies lower than the constructs without a construct at all. These authors also reported that there was no change in translational efficiency between different types of introns inserted into the construct. Related mRNA processing work carried out through microinjection of pre-mRNAs into *Xenopus* oocyte nuclei revealed that pre-mRNAs containing introns had greater percentages of export to the cytoplasm than the same pre-mRNAs without an intron (Luo and Reed 1999). These authors contributed this phenomenon to an exportation complex they detected on gels associating with only pre-mRNAs that contained introns. This exportation complex, called an exon-exon junction complex, was later found to contain at least five proteins (Le Hir et al. 2000) and to be directly responsible for the increased export efficiency of mRNAs with introns (Le Hir et al. 2001). Expressing the full length *AgNt84* gene *in planta* may address several issues in our current system. First, presence of introns could reduce *E. coli* toxicity seen during cloning of constructs putatively due to background expression of the metallohistin gene with its signal peptide. Secondly, low translational efficiency would explain the current conundrum in detecting ample amount of metallohistin mRNA in northern blots, but the inability to detect the presence of protein in western blots.

Current investigation of the full length *AgNt84* gene has been hampered by the large number of bands that appeared using primers specific to the cDNA. The multiple bands seen in the Nested PCR and the Southern blot probe suggest either one or a combination of three possibilities: 1) the metallohistin gene is a natural concatemer that

has several conserved repeats of varying length; 2) *AgNt84* represents only one cDNA in a larger family of genes that contain conserved regions; 3) the primers specific to *AgNt84* are also amplifying products from the homolog *AgNt164* or nonspecific genomic DNA. Because of the sequence similarity between *AgNt84* and *AgNt164*, the PCR primers specific to *AgNt84* could have amplified products from both genes giving the pattern of multiple bands. A sequence that matched the 5' UTR and coding region of *AgNt84* and *AgNt164* has been isolated. It could not be determined which cDNA the gDNA sequence matched to due to the strong sequence similarity of *AgNt84* and *AgNt164* at the 5' end and the mixed bases of the gDNA. Isolation and sequencing of the rest of the *AgNt84* or *AgNt164* gene will reveal which cDNA is being amplified from genomic DNA as *AgNt164* exhibits a 27 bp and 10 bp deletion that is not seen in *AgNt84*. Sequence similarity ends at a GT base pair region which could be the beginning of an intron sequence that cannot be predicted because it is longer than the portion of gDNA amplified and sequenced here. Two primer sets specific to *AgNt84* will amplify the full intron and the remaining coding region and any further introns that may be present. Only sequence greater than 1186 bp as the gDNA sequence matches to 179 bp of *AgNt84* 5' UTR and coding region and then has a potential intron that is a minimum of 531 bp which leaves 476 bp of the 3' coding region and UTR assuming no more introns are present.

The multiple bands exhibited in nested PCR reactions could be a result from nonspecific binding of primers or areas of repeated sequences in genomic DNA. In

addition, clean sequence could only be derived from using *AgNt84*-1 forward primer on the 1.2 kb gDNA band suggesting that the reverse primer was amplifying a non-specific area inside of a putative intron.

Currently, investigation into the possibility of the metallothionein gene being a natural concatemer is underway. Sequencing results from the remaining six bands of interest have come back muddled with multiple products and short reads. This is possibly because of the primers priming at several points within one PCR product rather than specifically to the 5' and 3' ends. This is further supported by the fact that multiple bands lengths ranging from 3.0 to 0.75 kb can be amplified from one gel extracted PCR product during nested PCR.

Future research will focus on characterization of T₂ homozygous *AgNt84* cDNA fragment *Nicotiana tabacum* plants, discovering the full length *AgNt84* gene, and assessing metal-binding ability in all transgenic *AgNt84* plants. Further investigation into the molecular biology of the metallothionein mRNA and full characterization of the role *AgNt84* plays *in vitro* and *in vivo* could lead to advances in phytoremediation and nitrogen-fixing microbe-plant interactions.

Chapter Three: SEM and TEM Characterization of

***Pteris vittata* Callus Induction and Regeneration**

Introduction

The fern *Pteris vittata*, also known as Chinese brake fern, belongs to the family Pteridaceae in the class Polypodiopsida. *Pteris vittata* has been classified as an arsenic hyperaccumulator capable of storing arsenic in fronds to 2.3% dry weight (Ma et al. 2001). To date, several members of the *Pteris* genus such as *Pteris cretica*, *Pteris umbrosa*, and *Pteris longifolia* have been described as arsenic hyperaccumulators (Zhao et al. 2002). In recent years the interest in using plants as sensors and remediators for real-time detection of pathogens (Mazarei et al. 2008b) and environmental contaminants (Ellis and Salt 2003; Muthukumar et al. 2007) has grown. Phytosensors and remediators would provide farmers and industry with cost effective, solar-powered, in-field tools to streamline the economic inputs and environmental impacts from agricultural and industrial processes through optimization of farming practices such as fertilizer and pesticide application, mitigation of yield reduction due to pathogens, and removal of toxic byproducts mobilized into the environment from industries such as mining, metal production, and chemical manufacturing.

Creation of phytosensors, however, requires genetic transformation of target organisms with elements capable of responding to the signal of interest. Through the years, an extensive amount of work has been accomplished with monocot, dicot, and

bryophyte tissue culture and transformation, but relatively little attention has been focused on pteridophytes. Early work on fern tissue culture focused primarily on conditions necessary for initiation of each life cycle stage. Multiple environmental and culture conditions such as the carbon source, osmotic potential, and light wavelength have been found to play roles in *Pteris* spore germination, gametophyte development, callus induction, and sporophyte production (Crotty 1967; Kato 1967; Sugai 1968; Kato 1969; Kato 1970; Prada et al. 2008).

Germination occurs when the rhizoid initial emerges from the spore. The protonema initial divides during this time and later develops into the gametophyte (Figure 5). After about four weeks sexual organs start to develop (Raghavan 1989). *P. vittata* is homosporous, meaning that its gametophyte produces both antheridia and archegonia. Antheridia, sperm producing structures, are almost always found on the top of the gametophyte whereas the archegonia, the egg producing structures, are typically found on the underside of gametophytes. Once fertilization occurs, the nuclei of the sperm and egg fuse and the embryo begins to divide. Fern sporophytes develop within a fertilized archegonium. The cell mass at the base of the sporophyte, called the foot, develops in the archegonial chamber and absorbs nutrients from the gametophyte during sporophyte development. The sporophyte becomes free-living when a root and shoot system develop, and the gametophyte dies.

There have been several reports of callus induction from *Pteris vittata* tissue (Kato 1963; Kshirsagar and Mehta 1978; Kwa et al. 1991; Trotta et al. 2007; Yang et al.

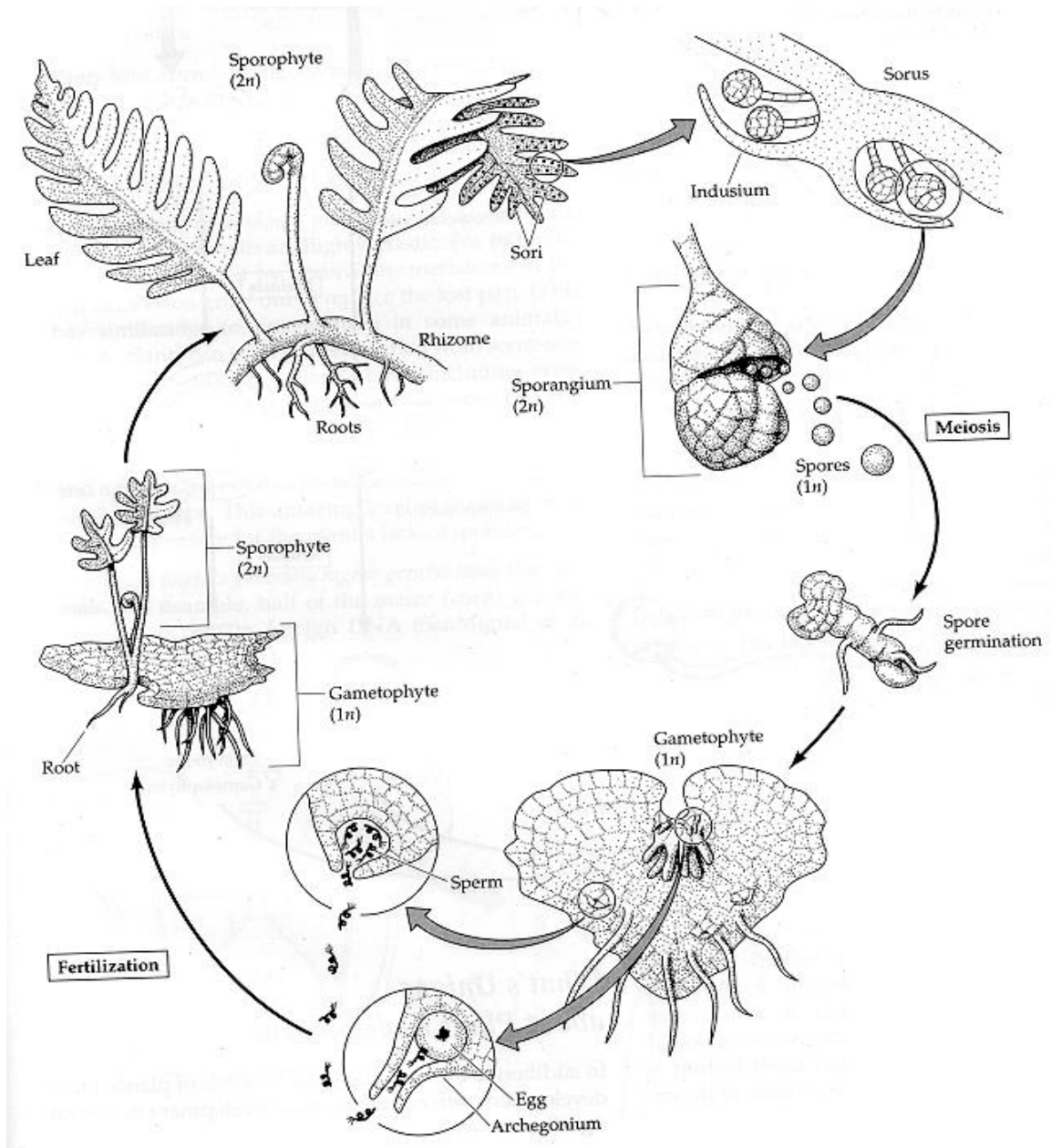


Figure 5. A diagram depicting the life cycle of ferns. Spores (1n) developed from sporophytes (2n) germinate and form gametophytes (1n). These gametophytes produce archegonia and antheridia which produce egg and spermatozoa sex cells. Fusion of these sex cells leads to formation of the sporophyte. Photo from http://www.esu.edu/~milewski/intro_biol_two/lab_2_moss_ferns/Fern_life_cycle.html.

2007). Callus formation has occurred on gametophytic tissue, croziers, rhizomes, and pinnae strips. In general, calli regenerated in the same life cycle of the tissue from which it was created. However, the calli produced from gametophytes in the tissue culture system described by Yang et al. (2007) recovers as sporophytic plants.

To date there have been no reports of *Pteris vittata* genetic transformation and little development of requisite tissue culture systems. However, biolistic transformation of *Ceratopteris richardii* gametophytes has been demonstrated, but only 7% of gametophytes were able to transfer the introduced genes to sporophytes (Rutherford et al. 2004). No sporophytes survived past the early development and so fern transformation techniques in general remain largely uncharacterized. A great problem in developing tissue culture systems *de novo* is ill defined tissue stages; i.e., not knowing if proliferating tissue is callus, somatic embryos or other differentiated tissue.

Scanning electron microscopy (SEM), transmission electron microscopy (TEM), and histology have been used to characterize tissue culture systems (Basu et al. 1997; Ovečka and Bobák 1999; Eudes et al. 2003; Namasivayam et al. 2006) as well as the fern life cycle (Gantt and Arnott 1965; Elmore and Adams 1976; Sheffield et al. 1983; Duckett and Ligrone 2003; Whittier 2003; Bondada et al. 2006). This work seeks to characterize the *Pteris vittata* callus induction, maintenance, and subsequent recovery of calli through use of light microscopy, transmission and scanning electron microscopy. Two conditions of callus induction, three conditions for callus maintenance, and two conditions for callus differentiation into sporophytes will be compared.

Materials and Methods

Environmental conditions and tissue culture

Two environmental conditions were used: light and dark. The lit environment had 16 hours of light at $79 \mu\text{mol m}^{-2} \text{s}^{-1}$ and 8 hours of darkness. The dark environment had 24 hours of darkness. Both environments had a constant temperature of 25 °C.

Spores were harvested from mature *Pteris vittata* fronds using a straight-edged razor blade and collected into 1.7 ml centrifuge tubes (Denville). They were then sterilized by soaking in a 10% dilution of sodium hypochlorite (5.25% sodium hypochlorite, Fischer Scientific) and then immediately centrifuging the tubes for 30 s. at 8,100 rcf. This was followed by suspending the spores in 70% ethanol and immediately centrifuging the tubes for 30 s. at 8,100 rcf. They were then rinsed three times with sterile water and plated onto half-MSO medium which contained 0.5 Murashige-Skoog salts (Murashige and Skoog 1962), B5 vitamins (Gamborg 1968), 2.0% sucrose, and solidified with 0.2% Gelrite gellan gum (Sigma). Plates of sterilized spores were placed in lit conditions to germinate. After about four weeks gametophytes formed and were transferred onto callus induction medium containing 0.5 MS salts, B5 vitamins, 2.0% sucrose, solidified with 0.2% Gelrite gellan gum supplemented with 0.5 mg L^{-1} 6-benzylaminopurine (BAP) and 0.5 mg L^{-1} gibberellic acid (GA_3) modified from Yang *et al.*, 2007. The plates were split and placed in either lit or dark conditions. Every two weeks the gametophytes were subcultured until they form calli. Calli were excised and subcultured and maintained on the same medium in the same conditions or on callus

induction medium lacking Gelrite gellan gum in dark conditions.

To induce differentiation, calli were moved to medium containing half-strength MS salts supplemented with 6.0% maltose (Fisher), 0.5% activated charcoal (Sigma), and solidified with 0.2% Gelrite gellan gum. The calli were placed in either the lit or dark conditions and subcultured onto new differentiation medium every two weeks. After six weeks, calli with sporophytic leaves were moved to the original MSO medium to root.

Fixation

Fifteen samples from each stage of tissue culture were randomly selected and put into 3% glutaraldehyde in 0.1M cacodylate buffer for 90 min. at room temperature. They were then rinsed three times in the cacodylate buffer and transferred to 2% OsO₄ in 0.1M buffer for 90 min. The samples were then dehydrated in a grade acetone series (25%, 50%, 75%, 95%, 100%, and dry 100%) for 30 min. at each step. The samples were then divided into two groups according to preparation needed for the scanning or transmission electron microscope.

Scanning Electron Microscopy

Samples were prepared using the critical-point drying method with carbon dioxide. Each tissue sample was affixed to two-sided carbon tape and then coated with 50 nm of gold. At least five samples were viewed from each stage of tissue culture and tissue culture condition.

Transmission Electron Microscopy

Samples were transferred into a 1 to 3 acetone/Spurr mixture overnight. The samples were then moved to a 3 to 1 acetone/Spurr mixture for 4 h. with the beaker lid on and 4 h. with the beaker lid removed. The samples were then placed into a 100% Spurr mixture and left overnight. Individual callus pieces were put into molds with fresh Spurr resin and placed in a 68 °C oven for 24 h to for Spurr blocks. At least three blocks for each condition were randomly selected and trimmed for thin-sectioning with glass knives on a microtome. Multiple sections were cut at a time and picked up on copper grids coated with glue. All grids were post-stained with uranyl acetate in 50% methanol for 30 min., and washed by dipping them 30 times into three different beakers of water. They were then stained in lead citrate for 5 min., washed again and then loaded for viewing.

Results

Callus induction in lit versus dark conditions

Gametophytes grown on callus induction medium in dark conditions developed rhizoids and callus (Figure 6A). Gametophytes grown in lit conditions swelled noticeably and produced callus with minimal rhizoids (Figure 6B). Callus induced and maintained in dark conditions were pale white (Figure 6C) whereas callus induced in lit conditions were yellowish-green (Figure 6D). White callus induced and maintained under dark conditions turned yellow-green after a culturing in lit conditions for a week

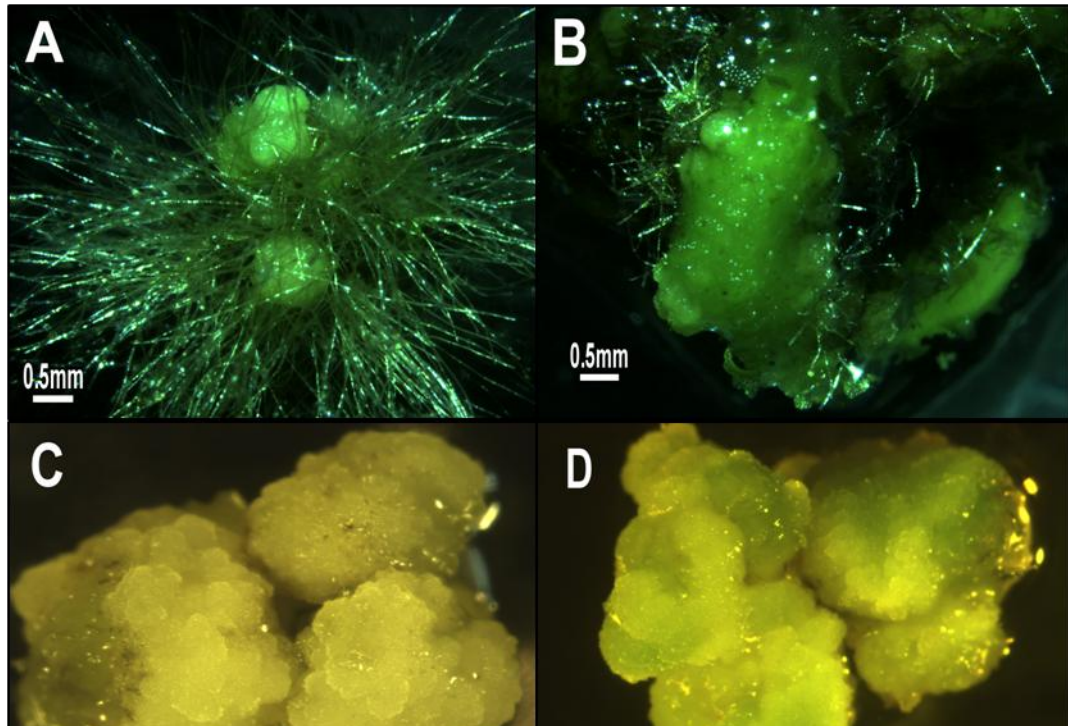


Figure 6. Light microscopy of gametophytes and callus grown on callus induction medium under dark (A & C) and lit conditions (B & D). A) Gametophytes grown in dark conditions produced rhizoids and callus. B) Gametophytes grown in lit conditions swelled and produced callus with minimal rhizoids. C) Callus maintained in dark conditions was pale white. D) Callus either moved from lit conditions or maintained under lit conditions were bright yellow-green.

(data not shown). Gametophytes began to swell after four to six weeks of culturing on callus induction medium (Figure 7A). Adventitious gametophytes, antheridia, archegonia, and a small number of rhizoids were present on the surface of the gametophyte after six weeks of culture on callus induction medium in lit conditions (Figure 7A, 5B, and 5C). Rhizoids were observed elongating in a radial pattern from the basal cells of antheridia-like structures (Figure 7D). Undifferentiated cells forming callus were present on the surface of gametophytes at eight weeks (Figure 7E). An extracellular matrix as well as fibrillar and granular structures were present on clusters of developing calli (Figure 7G and 5H).

Gametophytes cultured on callus induction medium in dark conditions also formed adventitious gametophytes (Figure 8A). Rhizoids were found universally on gametophytes cultured in dark conditions (Figure 8B, 6C, and 6D). Rhizoids were formed from antheridia-like structures and directly from the gametophyte surface (Figure 8B and 6D). Rhizoids were covered in fibrillar and granular structures during formation (Figure 8C). Calli developed at eight weeks (Figure 8E). Fibrillar structures were also found on dividing callus clusters (Figure 8F). Removal of rhizoids was necessary to view the entire surface of gametophytes grown on semi-solid medium under dark conditions. Large clusters of callus went undetected because of the dense network of rhizoids (Figure 8G). The surface of some calli had trichome-like structures (Figure 8H).

Maintenance of callus on semi-solid and liquid medium

Callus grew rapidly on both semi-solid and liquid medium. Callus browned or

Figure 7. Scanning electron microscopy of *Pteris vittata* gametophytes grown under lit conditions for six weeks (A & B) and eight weeks (C-H). A) Swollen gametophyte with adventitious gametophyte blades, rhizoids, and sex organs. B) Properly formed archegonia and antheridia on the gametophyte epidermis. C) Early formation of adventitious gametophytes and rhizoids from antheridia-like structures. D) Later stage of adventitious gametophyte formation and rhizoid production from antheridia-like structures. E) Formation of undifferentiated callus cells on the gametophyte epidermis. F) Extracellular matrix (ecm) covering dividing callus. G) Fibrillar and granular structures on dividing callus. H) Overview of fully formed and dividing callus.

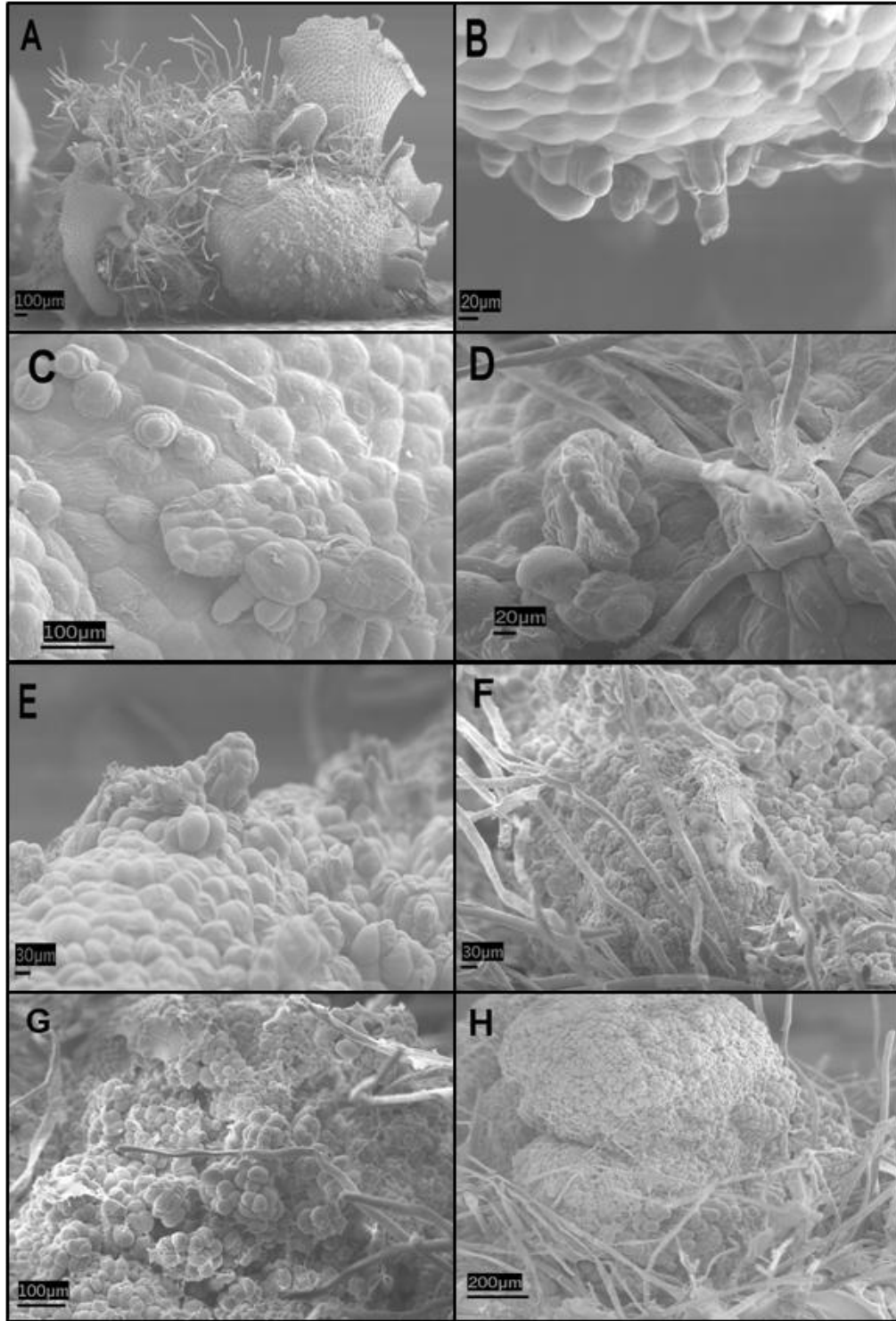


Figure 7. Continued.

Figure 8. Scanning electron microscopy of *Pteris vittata* gametophytes grown on callus induction medium in dark conditions for six weeks (A) and eight weeks (B-H). Rhizoids were removed to improve observation of dark grown gametophytes (G & H). A) Gametophytes grown in dark conditions for six weeks developed adventitious gametophyte blades. Rhizoids are present on all gametophytes grown in dark conditions. B) Rhizoids are produced from antheridium-like structures. C) Fibrillar and granular structures cover emerging rhizoids. D) Rhizoids, antheridia and archegonia on the gametophyte surface. E) Early callus dividing on epidermis of gametophyte. F) Fibrillar structures connect growing callus. G) Clusters of calli were observed once the majority of rhizoids were removed. H) Trichome-like structures indicative of sporophyte formation were present on some callus.

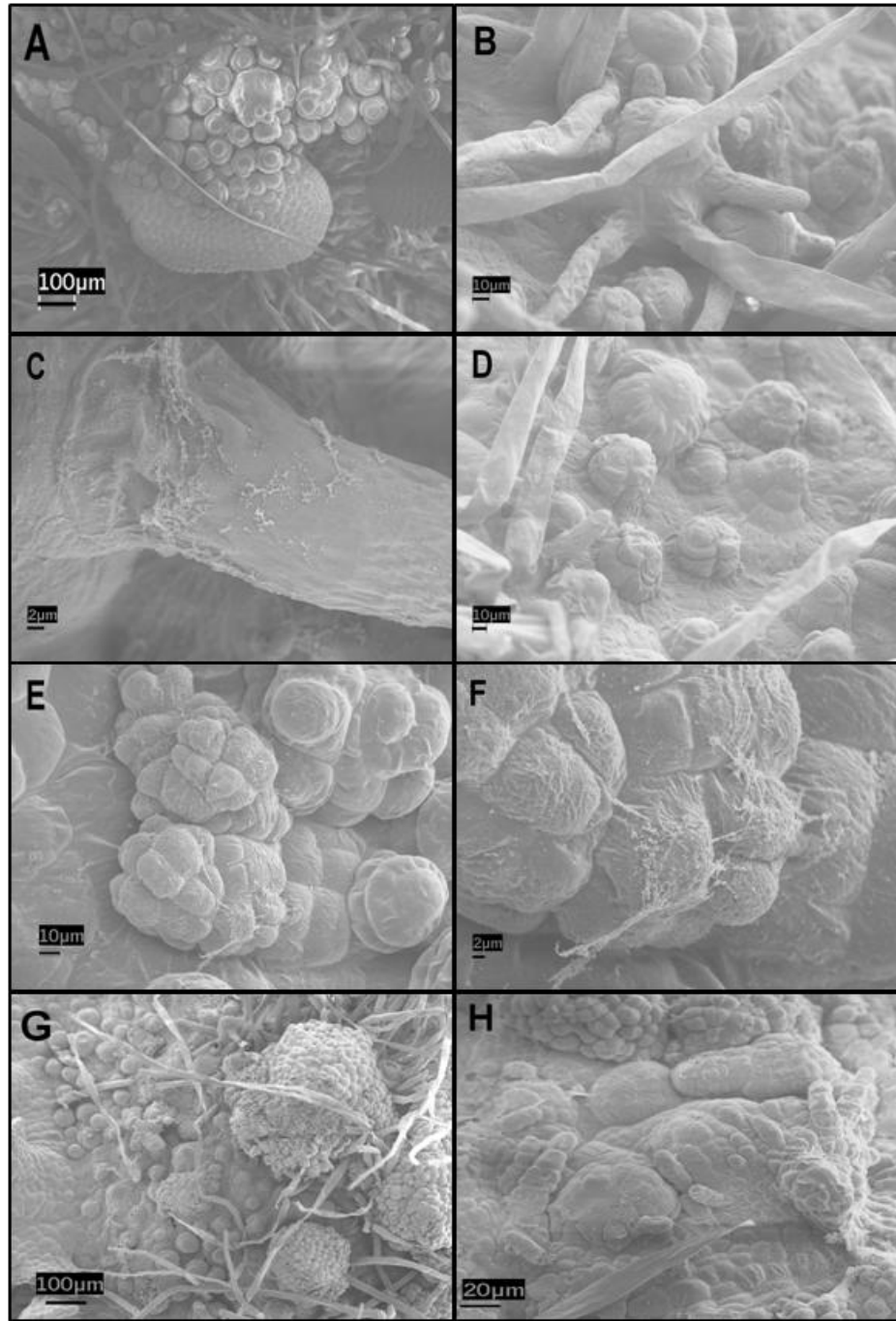


Figure 8. Continued.

started to differentiate if they were not subcultured every two weeks on semi-solid medium or every week on liquid medium. Plasmodesmata were prominent between cell walls of calli grown on semi-solid callus induction medium under lit conditions (Figure 9A). Golgi aparati were seen near the edges of cells and vesicles nearby were fused to the plasmalemma (Figure 9B). Multiple vacuoles and lipid microbodies associated with endoplasmic reticulum were in the central parts of cells (Figure 9B). Compared to cells of calli grown on semi-solid and liquid medium under differentiate if they were not subcultured every two weeks on semi-solid medium or every week on liquid medium. Plasmodesmata were prominent between cell walls of calli grown on semi- dark conditions, cells of calli grown on semi-solid medium under lit conditions were smaller (Figure 9C). The cells also had nuclei containing two nucleoli and turbidity in protein microbodies.

Less pronounced plasmodesmata were present in cell walls of calli grown on semi-solid medium in dark conditions as well as large central vacuoles with protein and lipid microbodies that dominated the cells (Figure 9D). Extensive invaginations of the cell wall contained vesicles (Figure 9E). Scanning electron microscopy revealed distinct nodules of cells on the surface of callus with an extracellular matrix and fibrillar structures connecting the structures (Figure 9F).

Large vacuoles with lipid microbodies surrounded by only a small amount of cytoplasm were present in cells of calli grown in liquid medium in dark conditions (Figure 9G). Nuclei with two nucleoli were also present in calli grown in liquid (Figure 9H). The surface of calli grown in liquid medium was made of broad cells undergoing division that did not have an extracellular matrix (Figure 9I).

Differentiation of callus into sporophytes

The average number of calli with sporophytes after one month and average number of sporophytes per callus for the two media types used are recorded in Table 3. Calli grown on MSM6AC differentiation medium under lit conditions began to form sporophytic leaves after three weeks. Callus multiplied readily on previously described regeneration medium (Zheng et al. 2008), but no regenerated sporophytes could be obtained. Calli grown under dark conditions did not differentiate into sporophytes. Scanning electron microscopy revealed trichome-like structures present on callus and differentiating sporophytes (Figure 10A). Emerging sporophytes were covered in trichome-like structures and more developed also had the trichome-like structures to a lesser extent (Figure 10B). An extracellular matrix extended across the cells just below the developing sporophytes in Figure 10B. Differentiation of sporophytic fronds from calli was nonsynchronous like callus induction from gametophytes (Figure 10C). An extracellular matrix and trichome-like structures marked developing sporophytes (Figure 10D).

Figure 9. Transmission electron microscopy and scanning electron microscopy of *Pteris vittata* callus maintained on semi-solid callus induction medium in lit (A, B, & C) and dark (D, E, & F) conditions and liquid medium in dark conditions (G, H, & I). A) Plasmodesmata were observed in calli grown on semi-solid callus induction medium under lit conditions. B) Presence of multiple small vacuoles, vesicles fused to the plasmalemma, endoplasmic reticulum associated with lipid microbodies, and golgi apparatus. C) Relatively smaller cells connected by plasmodesmata, multiple vacuoles, nuclei with two nucleoli, and turbidity in protein microbodies. D) Large central vacuoles with protein and starch microbodies in calli grown on semi-solid medium under dark conditions. Less prominent plasmodesmata were present in cell walls. E) Invaginations in the cell wall containing vesicles. F) Callus covered in distinct nodules of cells connected with extracellular matrix. G) Large vacuoles containing lipid microbodies with minimum cytoplasm in calli grown in liquid medium under dark conditions. H) Nucleus containing two nucleoli. I) Callus grown in liquid medium comprised of broad cells undergoing division. No extracellular matrix was observed on calli grown in liquid medium.

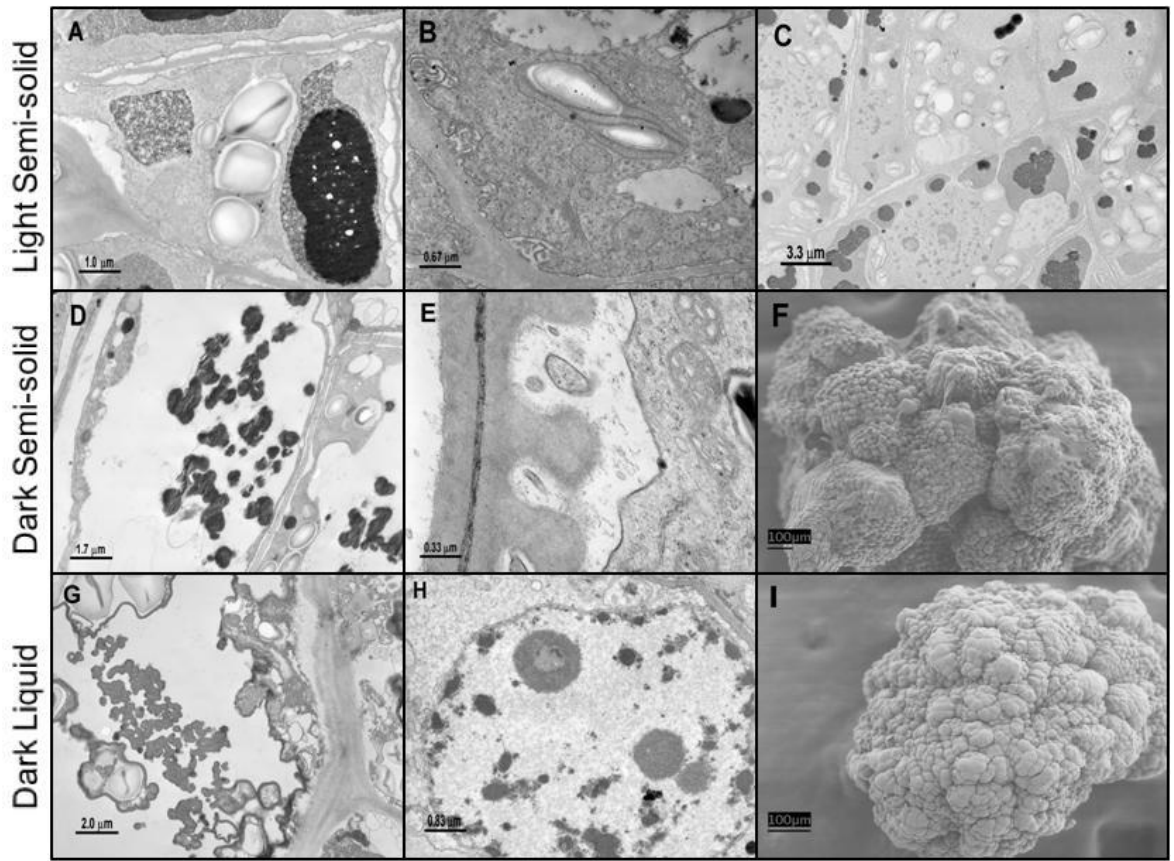


Figure 9. Continued.

Table 3. The ratio of *Pteris vittata* callus with differentiating sporophytes (regeneration efficiency) and average number of sporophytes per callus after one month on two media types.

Medium and Culture Condition	Regeneration Efficiency*	Sporophytes per Callus*
Light MSM6AC	38 ± 0.22%	3.92 ± 0.02
Dark MSM6AC	68 ± 13.5%	2.59 ± 0.55
Light Zheng	0.0%	0
Light Zheng	0.0%	0

* Each value represents the mean of three replicates of 25 individual callus ± standard deviation

Discussion

Previous work has described tissue culture systems that induce callus from *Pteris vittata* pinnae strips, rhizomes, croziers, and gametophytes. These reports typically focus on culture conditions and nutritional requirements necessary for tissue culture, but fail to fully characterize the events occurring during development, maintenance, and differentiation of callus. Understanding of these events is as important as tissue culture requirements to create *de novo* transformation protocols. Strangely, antheridia and archegonia were produced on both sides of the gametophytes during callus induction rather than being separated on two different parts of the gametophyte as in nature. In dark conditions, rhizoids were formed in thick mats over the entire surface of the gametophyte, but this has been observed in other *Pteris vittata* tissue culture systems. Calli induced from rhizomes produced “hairs” and sporophytic leaves on medium containing either low (1%) sucrose or high (4%) sucrose (Kshirsagar and Mehta 1978). Ubiquitous production of rhizoids and sex organs has been seen in other axenically culture fern gametophytes as well (Elmore and Adams 1976).

It is likely that induction of rhizoids and sex organs can be affected by culture conditions and growth hormones. Gibberellic acid has been shown to induce the formation of antheridia in the fern *Anemia phyllitidis* (Kaźmierczak 2003). More

Four Weeks

Eight Weeks

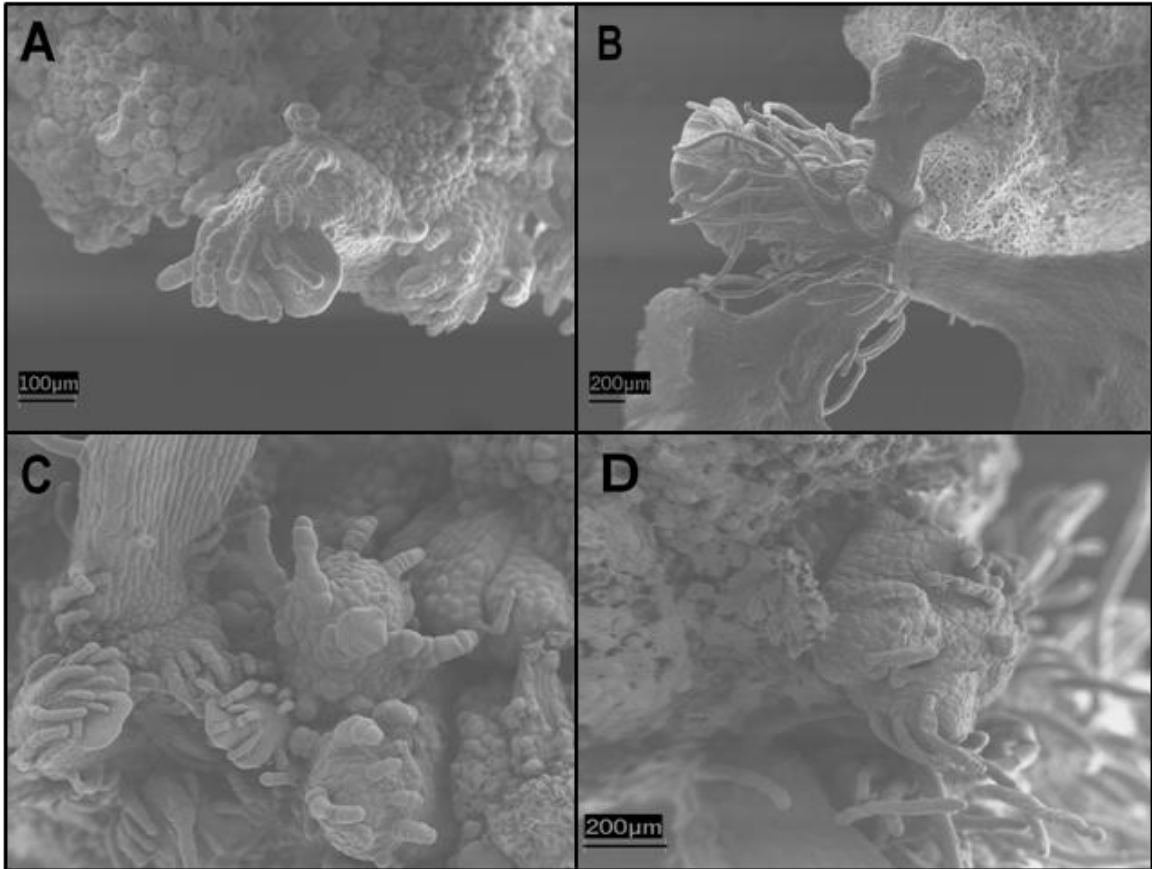


Figure 10. Regenerating callus grown on differentiation medium under lit conditions for four weeks (A & C) and eight weeks (B & D). A) Young sporophyte emerging from callus. Trichome-like structures appeared on callus and attached to the developing sporophytes. B) A crozier and maturing sporophytic fronds. Trichome-like structures are more noticeable on young sporophytic fronds, but are also present on more developed sporophytic fronds. Note extensive extracellular matrix just below developing sporophytes, and the crozier, the meristematic center of the sporophytes. C) Differentiation of sporophytes from callus is asynchronous. D) Trichome-like structures and extracellular matrix marking the site of a developing sporophyte.

precisely, GA₃ and ethylene interact to induce formation of antheridia (Kaźmierczak 2007). Presence of GA₃ in the medium and production of ethylene in sealed Petri dishes could account for the ubiquitous presence of antheridia and rhizoids. Typically, the cap cells of antheridia open to release spermatozoa for fertilization, but no opened antheridia were observed on any gametophytes in the current work suggesting no fusion of sex cells. Callus was observed forming on the epidermis of swollen gametophytes after eight weeks though the exact cell type that produced it could not be determined. It is unlikely callus was derived from antheridia or embryos formed from sexual reproduction. To optimize the tissue culture conditions and reduce presence of rhizoids and antheridia, growth under lit conditions and use of a micropore tape that allows for gas exchange to reduce concentrations of ethylene is recommended.

Callus development from archegonial cells or epidermal cells through as observed most likely occurs through apogamy. *Pteris cretica*, a fern related to *Pteris vittata*, also exhibits arsenic accumulation and reproduces through obligate apogamy. A transmission electron microscopy study revealed that the cells undergoing oogenesis had normal ultrastructural development characteristics inside *Pteris cretica* archegonia (El Desouky et al. 1990). As was seen in transmission electron micrographs the *Pteris vittata* callus cells during this work, developing *Pteris cretica* egg cells had a large number of free ribosomes, lipid bodies, many small vacuoles rather than a large central vacuole, and nuclei with diffuse chromatin and two nucleoli. This provides ultrastructural evidence that callus could develop from unfertilized egg cells.

Investigation of a moss *Physcomitrium coorgense* revealed that callus cells derived from gametophytes accumulated large amounts of starch and contained an abundant number of plasmodesmata just before forming apogamous sporophytes (Lal and Narang 1985). The sporophytes developed from superficial cells with “labyrinthine” cell walls that later became embedded in the callus due to growth of surrounding cells. All callus had large amounts of starch microbodies, but only the callus on semi-solid medium exhibited plasmodesmata connecting cells. Deep cell wall crenellation was observed in callus grown on semi-solid medium in dark conditions suggesting that these conditions may be the best for preparing callus to develop sporophytes. Overall, callus grown on semi-solid medium exhibited more mature apogamous ultrastructural characteristics than callus of the same age maintained on liquid medium. Callus maintained under dark conditions had a greater regeneration efficiency than callus maintained under lit conditions, however callus maintained under lit conditions produced more sporophytes per callus. It is difficult to determine which callus is more competent for regeneration because of the high degree of variability seen in dark grown callus. Callus maintained under dark conditions may be more suitable for regeneration as each callus has a greater chance to produce at least one sporophyte, but further replicates are needed.

Scanning electron microscopy revealed that callus grown on semi-solid medium had distinct nodule structures of cells, whereas callus grown in liquid medium were made of cells that were larger and less distinct. Histology of *Pteris vittata* rhizome callus has previously revealed distinct nodules of meristematic cells which gave rise to shoots,

roots, or both depending on concentrations of sucrose and 2,4-D present in the medium (Kshirsagar and Mehta 1978). The callus from semi-solid medium also had an extracellular matrix present whereas the callus from liquid medium did not. This is the first report of an extracellular matrix seen on pteridophyte callus tissue. An extracellular matrix has been observed on tissue during embryogenesis and organogenesis in flowering plants such as *Coffea arabica* (Sondahl 1979), *Papaver somniferum* (Ovečka and Bobák 1999), *Brassica napus* (Namasivayam et al. 2006), and *Actinidia deliciosa* (Popielarska-Konieczna et al. 2008). Namasivayam et al. (2006) considered the presence of an extracellular matrix as a marker for tissue that has entered the pre-embryogenic state. In *A. deliciosa*, the extracellular matrix can be membranous, fibrillar, or granular and is made of low-esterified pectin and some lipophilic substances (Popielarska-Konieczna et al. 2008). It has been suggested that the extracellular matrix could play a role in cell-cell signal cascades to coordinate development of callus through an extracellular matrix-plasmodesmata-cytoskeleton continuum (Ovečka and Bobák 1999). These authors cited previous work in *Cichorium* (Hilbert et al. 1992) and on arabinogalactanproteins (AGPs) to support their claim. In *Cichorium*, two proteins were detected during embryogenesis and correlated to formation of external glycoprotein fibrillar networks (Hilbert et al. 1992). Some arabinogalactanproteins have been implicated in cell-cell signaling during cell proliferation by spatial and developmental regulation (Du et al. 1996). In this work, extracellular matrices were observed on callus tissue from the start of induction until differentiation. Notably, an extensive matrix was

observed on callus tissue at the base of differentiating sporophytes after eight weeks of culture on differentiation medium. Though possible functions of the extracellular matrix in pteridophytes are currently unknown, the theory that it is involved in cell-cell signal cascades to coordinate development is plausible due to its presence at the base of forming and differentiating callus. This would then suggest the callus induced on semi-solid medium would be regenerated more easily.

Though several tissue culture systems have been identified, only the method described by Yang (2008) induces callus from a gametophyte explant and produces a different portion of the fern life cycle, sporophytes. Typically, these two portions of the fern life cycle are separated by the diploid sporophyte stage. For example, croziers, a part of the diploid life cycle, have been used as explants to induce callus which differentiated into sporophytes (Trotta et al. 2007). Most ferns, however, can undergo a process called apogamy where sporophytes form without sexual reproduction which could account for sporophyte development from callus originally derived from haploid gametophytes.

In 1970, Kato found that apogamous sporophytes developed when *Pteris vittata* gametophytes were cultured on medium containing 0.5% - 2.0% sucrose or 1.0% - 2.0% glucose in the dark. Apogamous sporophyte formation was increased if casein hydrolysate, yeast extract, wheat germ extract, indole acetic acid, or tryptophan was added to the basal medium. As was seen in this work, Kato also observed gametophytes that “thickened” and produced vascular strands that did not become sporophytes on

sucrose medium under white light. Most likely, these vascular strands are the rhizoids observed in this work. Thickening of the prothalli has been considered a major step in the formation of apogamous sporophytes. When gametophytes of the fern *Pteridium* were grown on medium containing sugar the prothalli thickened and produced a mass of tissue that produced apogamous sporophytes (Whittier 1962). In the present work, thickened prothalli produced other prothalli in addition to callus that could be maintained for over a year on callus induction medium. This supports the claim of apogamous callus induction in this work.

Future work will focus on histology of gametophytes during callus induction and sporophytic differentiation is needed to pinpoint from which cells these structures arise. Further flow cytometry or chromosome squashes of gametophytes, calli, regenerated sporophytes, and sporophytes derived from spores will aid in characterizing the impact tissue culture plays on the life cycle and ploidy level of *Pteris vittata*. This is especially important as alterations of ploidy level in sporophytes could have interesting consequences for transgenic sporophytes and successive generations. Apogamous sporophytes in *Pteris multifida* rarely produced viable spores (Kawakami et al. 1995). When tetraploid *Pteris vittata* gametophytes were plated on Knudson's medium with 2.0% sucrose green callus formed after 10-12 weeks and later apogamous sporophytes were produced (Palta and Mehra 1983). These apogamous sporophytes, termed polyhaploid sporophytes, showed lower overall fertility when compared to normal tetraploid sporophytes. Some sporophylls, fronds that bear spore, exhibited complete

infertility while others exhibited mixed fertility and production of spores that were viable and had the correct chromosome number through endomitosis or complete asynapsis. Transgenic apogamous polyploid sporophytes that have reduced or no capability of producing viable spores could provide an interesting and novel method to control gene flow for phytosensors.

This work has characterized the *Pteris vittata* the complete tissue culture system originally described by Yang et al. (2008). Optimization of culture conditions and hormones is required to reduce occurrence of rhizoids and antheridia and maximize callus induction. Callus maintained on semi-solid medium showed the most promising ultrastructural and structural characteristics of regenerable callus when compared to liquid medium of the same age. Further histology and cytology is necessary to elucidate the precise origins of callus and sporophytes. The only obstacle perceivable in developing a transformation protocol for *Pteris vittata* by biolistic bombardment of gametophytes would be callus induction from surviving cells of gametophytes during culture on semi-solid medium with appropriate antibiotic selection. If callus can be induced from any transgenic epidermal cell capable of surviving selection, recovery of callus into sporophytes is rapid and requires only a simple medium.

Chapter IV: A Preliminary Investigation of Techniques for Genetic Transformation of *Pteris vittata*

Introduction

Genetic transformation of fern species has been largely overlooked. As stated in Chapter 3, there is only one report of genetic transformation of fern gametophyte tissue. To develop techniques for genetic transformation of *Pteris vittata* sporophytes both protoplast- and biolistic-mediated transformation systems have been considered.

Protoplast transformation techniques are attractive because protoplast isolation and recovery systems have been developed for *Pteris vittata* (Ito 1962; Kadota and Wada 1989). These systems, however, do not produce large quantities of protoplasts that would be needed for genetic transformation. Even though no genetic transformation has been attempted with fern protoplasts, techniques using polyethylene glycol (PEG) mediated transformation of *Nicotiana tabacum* protoplasts (Koop et al. 1996) have been developed.

Successful biolistic bombardment techniques have been developed for a wide range of plant species and tissue types for both transient and stable transgene expression. A biolistic technique has even been successfully used to transform gametophytes of *Ceratopteris richardii* with GUS constructs (Rutherford et al. 2004). Biolistics, therefore, is the more attractive technique even though it requires extensive optimization. It is still not known which promoters can effectively drive transgene expression in ferns.

Both protoplast and biolistic bombardment techniques also benefit from the ease associated with which plasmids containing different promoters can be employed.

The ultimate goal of *Pteris vittata* genetic transformation is production of transgenic sporophytes capable of detecting arsenic and reporting with a fluorescent protein. In order to achieve this goal, this work seeks to establish a genetic transformation technique to produce transgenic *Pteris vittata* sporophyte lines.

Materials and Methods

Tissue culture of *Pteris vittata*

Tissue culture conditions and media for spore germination and callus induction were performed as described in Chapter 3. *Pteris vittata* sporophytes used for controls were maintained in a greenhouse at 32 °C for 16/8 h light/dark photoperiods.

Protoplast isolation

The digestion enzyme solution (1.0% cellulose R-10 (bioWORLD), 0.75% macerozyme R-10 (bioWORLD), 0.6M mannitol and 10 mM MES pH 5.7) was prepared fresh for each extraction. This solution was placed in a 55 °C waterbath for 10 minutes. The solution was then removed and allowed to cool to room temperature. Then 0.1g of bovine serum albumin fraction V (Sigma), 27 µl of a 1.25M CaCl₂ stock, and 34 µl of 5 mM β-mercaptoethanol (Sigma) were added to each 100 ml of the digestion enzyme solution and mixed to dissolve.

Fronds from sporophytes were collected and weighed. Pinnae strips were stacked and cut into thin strips in 20 ml of the above digestion enzyme solution contained in a glass Petri dish. All pinnae strip sections were kept in the dark while shaking. If vacuum infiltration was used the Petri dishes were placed in a Nalgene vacuum chamber for one hour while shaking, and then removed to complete digestion. Separate trials to optimize digestion time from 1, 2, 3, 4, 5, and 15 h were carried out. The resulting solution of protoplasts and cellular debris were filtered with either a 40 or 70 μm nylon cell strainer (BD Falcon) and collected.

Protoplast solutions were collected in a 50 ml Falcon tube and centrifuged in a Beckman Coulter Avanti J-E floor centrifuge at 150 rcf for 5 min at 25°C. Sucrose gradients ranging from 0.5 to 1.0 M were also tested during centrifugation. After protoplast isolation, 10 μl samples of the protoplast solution were dyed with Evan's blue to assay plasmalemma viability. Viable protoplasts were counted using a hemacytometer.

Biolistic bombardment of induced callus

Roughly 500 mg of calli were arranged in the center callus induction medium plates for biolistic transformation. *Pteris vittata* fronds, *Nicotiana tabacum* cv. *Xanthi*, and *Oryza sativa* leaf controls were also arranged in the same area at the center of medium plates containing only agar as controls for biolistics. To determine optimal conditions for shooting, plates were shot with 7929 kPa (1,150 psi) and 4482 kPa (650 psi) rupture disks as well as using 1.0 μm and 0.6 μm gold particles. GUS assays were

performed on calli three days post-shooting. Calli were put into GUS staining solution (50 mg X-GLUC, 5 ml DMSO, 10 ml 1M KPO₄, and 2 drops of Triton-X-100) for 24 hours at 37 °C. The GUS staining solution was then removed and 70% ethanol pipetted onto the calli every 12 hours to bleach the calli.

Calli and controls were shot with plasmids coding for green and red fluorescent proteins (GFP, RFP) with various promoters (Table 3) were viewed under an Olympus SZX12 stereo microscope with either 460-490 nm excitation and 535/40 nm emission filters or 520-550 nm excitation and 580 long pass emission filters respectively at 2, 3, 4, and 5 d post-shooting.

Results

Protoplasts

Protoplasts were successfully isolated from *Pteris vittata* gametophytes and sporophytic fronds (Figure 11A). Cellular debris and burst protoplasts were also present in extracted protoplasts (Figure 11A and 11B). A high level of autofluorescence was seen in protoplasts under the green fluorescent filter set (Figure 11C and 11D). An outline detailing the steps in protoplast extraction optimization from *Pteris vittata* tissues is presented in Figure 12. Digestion of sporophytes and gametophytes was typically completed after one hour of vacuum

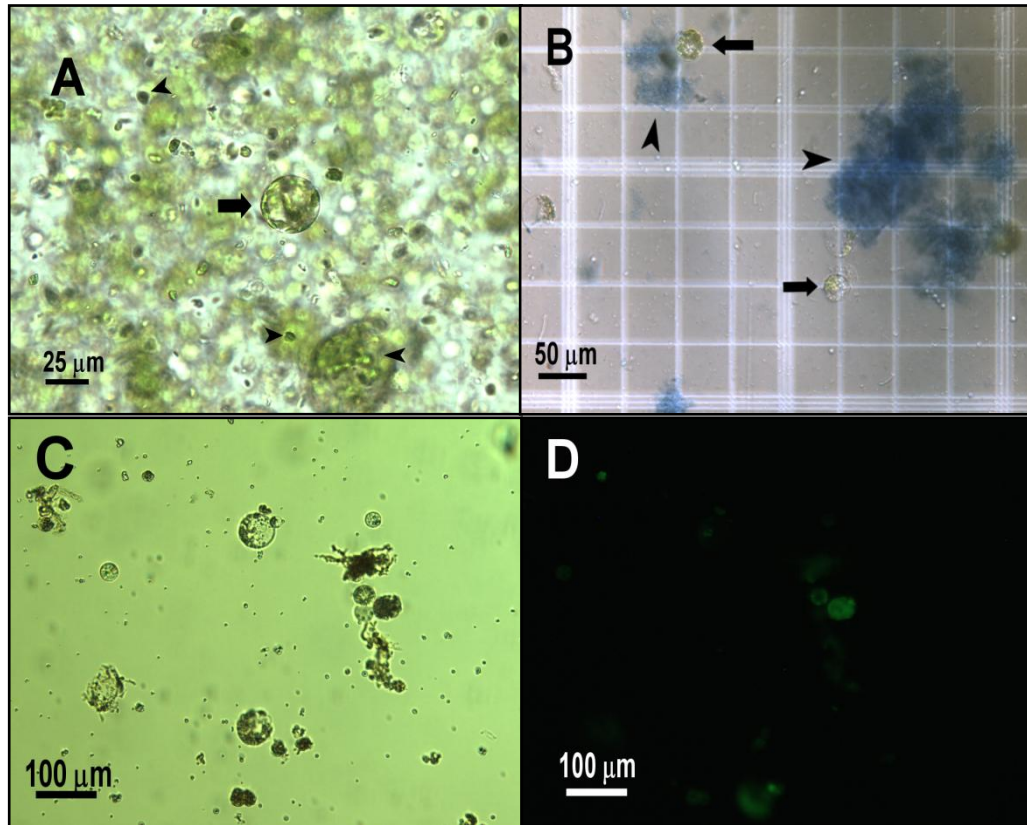
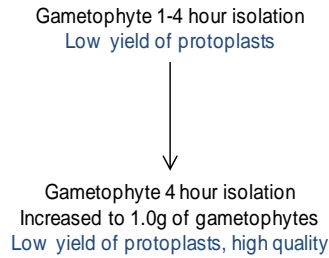


Figure 11. Protoplasts isolated from *Pteris vittata* sporophytes and gametophytes. A) Protoplasts (arrow) and cellular debris (arrowhead) from *Pteris vittata* sporophyte fronds. B) Gametophytic protoplast viability test using Evan's blue dye on a hemacytometer. Protoplasts (arrows) were often surrounded by large amounts of blue cellular debris (arrowhead). C) Bright field of protoplast isolated from sporophyte fronds. D) Autofluorescence seen in the same protoplasts under green fluorescence filters.

Gametophyte Tissue



Sporophyte Tissue

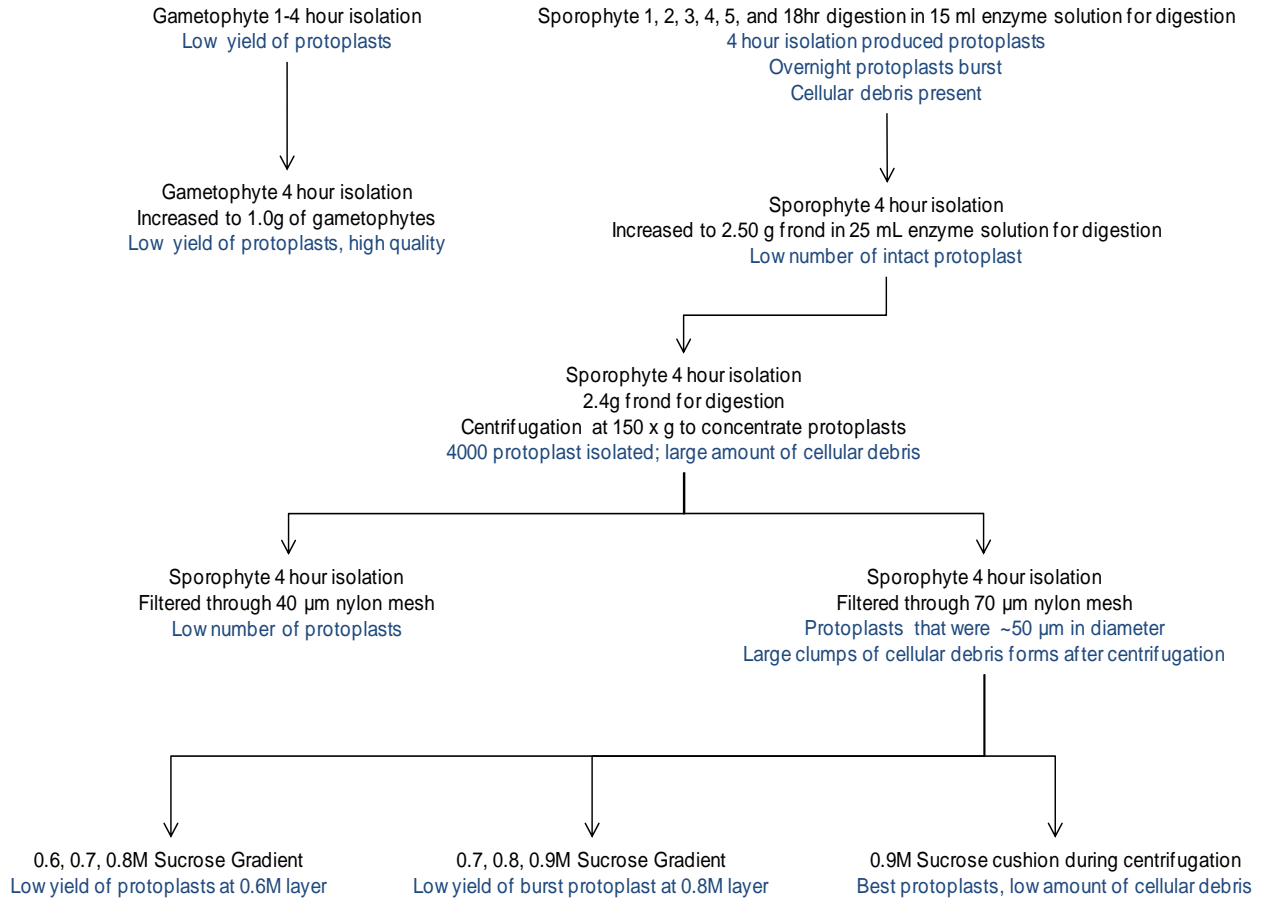


Figure 12. Flow chart of *Pteris vittata* protoplast isolation optimization. Experimental changes to the standard method are presented in black font and results are shown in blue font.

infiltration in digestion enzyme solution and three hours of shaking at 60 rpm. Centrifugation was necessary to concentrate the protoplasts to a countable amount. Masses of suspended cellular debris were observed after centrifugation steps containing only the filtered protoplast solution. Stepwise sucrose gradients reduced the formation of this cellular debris during centrifugation, but small numbers of protoplasts were typically seen at each layer. A single layer of 0.9 M sucrose beneath the protoplast solution reduced formation of the cellular debris and provided a layer of round protoplasts.

Biolistic bombardment

Gene expression was only detected in *Nicotiana tabacum* cv *Xanthi* controls. *Nicotiana tabacum* controls exhibited green fluorescence stronger than background autofluorescence with the appropriate GFP filters, but did not have autofluorescence detectable with RFP filters (Figure 13). Vectors and their promoters and marker genes as well as the number of plates of *Pteris vittata* callus and controls that were shot are recorded in Table 3. In constructs containing red (RFP) or green fluorescent

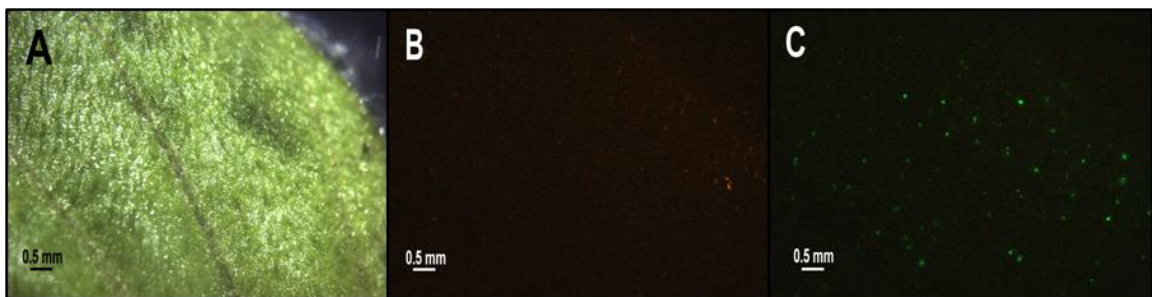


Figure 13. Transformation of *Nicotiana tabacum* cv. *Xanthi* controls with pAHC25-gfp5er. A) Bright field *Nicotiana tabacum* leaf. B) *Nicotiana tabacum* leaf under red fluorescent filters exposed for two minutes. No autofluorescence is observed. C) *Nicotiana tabacum* leaf under green fluorescent filters exposed for two minutes. Multiple spots exceed background autofluorescence.

Table 4. Tissue type, promoters and marker genes used in biolistic bombardment of *Pteris vittata* callus.

Tissue Type	Plasmid	Promoter	Marker gene	Number of Plates	Reference *
<i>Pteris vittata</i> callus	pAHC25- <i>gbr15</i>	Maize Ubiquitin 1	Gbr15 - RFP	6	1
<i>Pteris vittata</i> callus	pAHC25- <i>gfp5er</i>	Maize Ubiquitin 1	GFP5er – GFP	6	1
<i>Nicotiana tabacum</i> leaf	pAHC25- <i>gfp5er</i>	Maize Ubiquitin 1	GFP5er – GFP	2	1
<i>Pteris vittata</i> callus	pAHC25	Maize Ubiquitin	GUS	7	1
<i>Pteris vittata</i> frond	pAHC25	Maize Ubiquitin 1	GUS	2	1
<i>Nicotiana tabacum</i> leaf	pAHC25	Maize Ubiquitin 1	GUS	2	1
<i>Pteris vittata</i> callus	pRESQ70	Rice Ubiquitin	GUS	2	2
<i>Pteris vittata</i> callus	pRESQ101	Rice Ubiquitin	GUS	2	2
<i>Pteris vittata</i> callus	pMyGUS	Badna Streak Virus	GUS	2	3
<i>Pteris vittata</i> callus	pCvGUS	Badna Streak Virus	GUS	2	3
<i>Pteris vittata</i> callus	pMyGFP	Badna Streak Virus	SGFP	2	3
<i>Pteris vittata</i> callus	pCvGFP	Badna Streak Virus	SGFP	2	3
<i>Pteris vittata</i> callus	pSK-35S	Cauliflower Mosaic Virus 35S-S1	GUS	6	
<i>Pteris vittata</i> frond	pSK-35S	Cauliflower Mosaic Virus 35S-S1	GUS	2	
<i>Nicotiana tabacum</i> leaf	pSK-35S	Cauliflower Mosaic Virus 35S-S1	GUS	2	

* 1 - Christenson and Quail 1996; Sivamani and Qu 2006; Schenk 2001

proteins (GFP), no calli exhibited fluorescence stronger than background auto-fluorescence.

Discussion

Low numbers of extracted protoplasts and presence of cellular debris hindered the use of protoplasts for genetic transformation of *Pteris vittata*. Other fern protoplast isolation systems also yield low numbers of protoplasts. An optimized protocol for isolating protoplasts from *Lygodium japonicum* sporophytes yielded 1.07×10^4 protoplasts on average. In comparison, on average 6.00×10^5 protoplasts were isolated from the leaf tissue of the switchgrass cultivar Alamo, and 2.00×10^5 of those protoplasts were used for each transformation (Mazarei et al. 2008).

When considering continued effort on this technique for possible transformation of *Pteris vittata*, regeneration is essential. And so, it is crucial to note that *Pteris vittata* protoplasts isolated by mechanical chopping of tissue were capable of recovering as gametophytes (Ito 1962). If yields and purity could be improved, protoplast isolation and transformation would be an excellent technique to use for promoter expression efficiency screening and possibly even recovery of transformed gametophytes or sporophytes.

Biolistic transformation of *Pteris vittata* callus tissue did not produce noticeable amounts of GFP, RFP, or GUS activity. In the only example of its kind, *Ceratopteris richardii* gametophytes were transformed using biolistic bombardment with GUS

constructs driven by the cauliflower mosaic virus 35S promoter (Rutherford et al. 2004). It is important to note that the gametophytes were histologically stained 6 days after bombardment and showed expression. In this work, GFP and RFP constructs were assayed at five days after bombardment, but no bombardments were assayed six or more days after bombardment. For future transformation studies, GUS constructs will be focused on as lower levels of expression of GUS are more easily detected than in GFPs or RFPs. *Pteris vittata* gametophytes will be used as target tissue instead of callus. If expression of GUS can be observed in gametophytes, rounds of bombarded gametophytes can be plated on callus induction medium with selection in an effort to generate transgenic callus tissue for recovery of sporophytes.

References

References

- Acar, YB, and AN Alshawabkeh. 1993. Principles of electrokinetic remediation. *Environmental Science & Technology* 27 (13): 2638-2647.
- Baker, AJM. 1981. Accumulators and excluders – strategies in the response of plants to heavy metals. *Journal of Plant Nutrition* 3 (1-4): 643-654.
- Baker, AJM, RD Reeves, and ASM Hajar. 1994. Heavy-metal accumulation and tolerance in British populations of the metallophyte *Thlaspi caerulescens* (Brassicaceae). *New Phytologist* 127: 61-68.
- Basu, S, G Gangopadhyay, BB Mukherjee, and S Gupta. 1997. Plant regeneration of salt adapted callus of indica rice (var. Basmati 370) in saline conditions. *Plant Cell, Tissue and Organ Culture* 50: 153-159.
- Bendahmane, A, M Querci, K Kanyuka, and DC Baulcombe. 2000. *Agrobacterium* transient expression system as a tool for the isolation of disease resistance genes: application to the *Rx2* locus in potato. *Plant Journal* 21: 73-81.
- Blake II, RC, DM Choate, S Bardhan, N Revis, LL Barton, and TG Zocco. 1993. Chemical transformation of toxic metals by a *Pseudomonas* strain from a toxic waste site. *Environmental Toxicology and Chemistry* 12: 1365-1376.
- Bizily, SP, CL Rugh, and RB Meagher. 2000. Phytodetoxification of hazardous organomercurials by genetically engineered plants. *Nature Biotechnology* 18: 213-217.

- Bondada, B, C Tu, and L Ma. 2006. Surface structure and anatomical aspects of Chinese brake fern (*Pteris vittata*; Pteridaceae). *Brittonia* 58: 217-228.
- Brettschneider, R, D Becker, and H Lorz. 1997. Efficient transformation of scutellar tissue of maize embryos. *Theoretical and Applied Genetics* 94: 737-748.
- Briat, JF and M Lebrun. 1999. Plant response to metal toxicity. *Plant Biology and Pathology* 322: 43-54.
- Byers, H.G and HG Knight. 1935. Selenium in soils – In relation to its presence in vegetation. *Industrial and Engineering Chemistry* 27: 902-904.
- Campbell, DH. 1905. The homosporous Leptosporangiateae (Filices). In: *The Structure and Development of Mosses and Ferns (Archegoniatae)*. London, England: Macmillan 346-395.
- Canhoto, JM, JF Mesquita, and GS Cruz. 1996. Ultrastructural changes in cotyledons of pineapple guava (Myrtaceae) during somatic embryogenesis. *Annals of Botany* 78: 513-521.
- Chabregas, SM, DD Luche, MA Van Sluys, CFM Menck, and MC Silva-Filho. 2002. Differential usage of two in-frame translational start codons regulates subcellular localization of *Arabidopsis thaliana* TH11. *Journal of Cell Science* 116: 285-291.
- Chair, H, T Legavre, and E Guiderdoni. 1996. Transformation of haploid, microspore-derived cell suspension protoplasts of rice (*Oryza sativa* L.). *Plant Cell Reports* 15: 766-770.
- Chaney, RL, YM Li, SL Brown, FA Homer, M Malik, JS Angle, AJM Baker, RD Reeves, and M Chin. Improving metal hyperaccumulator wild plants to develop

- commercial phytoextraction systems: approaches and progress. In: Terry N, GS Bañuelos, eds. *Phytoremediation of Contaminated Soil and Water*. Boca Raton, FL: CRC Press 129-169.
- Chapman, A, A Blervacq, J Tissier, B Delbreil, J Vasseur, and J Hilbert. 2000. Cell wall differentiation during early somatic embryogenesis in plants. I. Scanning and transmission electron microscopy study on embryos originating from direct, indirect, and adventitious pathways. *Canadian Journal of Botany* 78: 816-823.
- Christensen, AH and PH Quail. 1996. Ubiquitin promoter-based vectors for high-level expression of selectable and/or screenable marker genes in monocotyledonous plants. *Transgenic Research* 5: 213-218.
- Clemens, S. 2006. Toxic metal accumulation, responses to exposure and mechanisms of tolerance in plants. *Biochimie* 88: 1707-1719.
- Coutu, C, J Brandle, D Brown, K Brown, B Miki, J Simmonds, DD Hegedus. 2006. pORE: a modular binary vector series suited for both monocot and dicot plant transformation. *Transgenic Research* DOI 10.1007/s11248-007-9066-2.
- Crotty, W. 1967. Rhizoid cell differentiation in the fern gametophyte of *Pteris vittata*. *American Journal of Botany* 54: 105-117.
- Curtis, M and U Grossniklaus. 2003. A Gateway cloning vector set for high-throughput functional analysis of genes in planta. *Plant Physiology* 133: 462-469.
- Cunningham, SD and WR Berti. 2000. Phytoextraction and phytostabilization: technical, economic, and regulatory considerations of the soil-lead issue. In: Terry N, GS

- Bañuelos, eds. *Phytoremediation of Contaminated Soil and Water*. Boca Raton, FL: CRC Press 129-169.
- Dahmani-Muller, H, F van Oort, B Gélie, and M Balabane. 2000. Strategies of heavy metal uptake by three plant species growing near a metal smelter. *Environmental Pollution* 109: 231-238.
- Deblaere, R, B Bytebier, H De Greve, F Deboeck, J Schell, M Van Montagu, and J Leemans. 1985. Efficient octopine Ti plasmid-derived vectors for *Agrobacterium*-mediated gene transfer to plants. *Nucleic Acids Research* 13: 4777-4788.
- Du, H, AE Clarke, and A Bacic. 1996. Arabinogalactanproteins: a class of extracellular matrix proteoglycans involved in plant growth and development. *Trends in Cell Biology* 6: 411-414.
- Duckett, JG, and R Ligrone. 2003. The structure and development of haustorial placentas in Leptosporangiate ferns provide a clear-cut distinction between Euphyllophytes and Lycophytes. *Annals of Botany* 92: 513-521.
- Ehsan, S, SO Prasher, and WD Marshall. Simultaneous mobilization of heavy metals and polychlorinated biphenyl (PCB) compounds from soil with cyclodextrin and EDTA in admixture. *Chemosphere* 68: 150-158.
- El Desouky, FA, SM Laird, and E Sheffield. 1990. Oogenesis in the apogamous fern *Pteris cretica*. *Annals of Botany* 65: 297-303.
- Elmore, HW, and RJ Adams. 1976. Scanning electron microscopic observations on the gametophyte and sperm of the bracken fern, *Pteridium aquilinum* (L.) Kuhn. *New*

- Phytologist* 76: 519-522.
- Ellis, DR and DE Salt. 2003. Plants, selenium and human health. *Current Opinion in Plant Biology* 6: 273-279.
- Ellis, DR, L Gumaelius, E Indriolo, IJ Pickering, JA Banks, and DE Salt. 2006. A novel arsenate reductase from the arsenic hyperaccumulating fern *Pteris vittata*. *Plant Physiology* 141: 1544-1554.
- Ernst, W.H.O. 1996. Bioavailability of heavy metals and decontamination of soil by plants. *Applied Geochemistry* 11:163–167.
- Eudes, F, S Acharya, A Laroche, LB Selinger, and KJ Cheng. 2003. A novel method to induce direct somatic embryogenesis, secondary embryogenesis and regeneration of fertile green cereal plants. *Plant Cell, Tissue and Organ Culture* 73: 147-157.
- Fan, TWM, AN Lane, J Pedler, D Crowley, and RM Higashi. 1997. Comprehensive analysis of organic ligands in whole root exudates using nuclear magnetic resonance and gas chromatography–mass spectrometry. *Analytical Biochemistry* 251: 57–68.
- Frérot, H, C Lefévre, W Gruber, C Collin, A Dos Santos, and J Escarré. 2006. Specific interactions between local metallophilous plants improve the phytostabilization of mine soils. *Plant and Soil* 282: 53-65.
- Gantt, E and HJ Arnott. 1965. Spore germination and development of the young gametophyte of the ostrich fern (*Matteuccia struthiopteris*). *American Journal of Botany* 52: 82-94.

- Gilmartin, GM. 2005. Eukaryotic mRNA 3' processing: a common means to different ends. *Genes & Development* 19: 2517-2521.
- Gupta, RK, SV Dobritsa, CA Stiles, ME Essington, Z Liu, CH Chen, EH Serpersu, and BC Mullin. 2002. Metallothioneins: a new class of plant metal-binding proteins. *Journal of Protein Chemistry* 21(8): 529-536.
- Holtorf, H, A Hohe, HL Wang, M Jugold, T Rausch, E Duwenig, and R Reski. 2002. Promoter subfragments of the sugar beet V-type H⁺-ATPase subunit c isoform drive the expression of transgenes in the moss *Physcomitrella patens*. *Plant Cell Report* 21: 341-346.
- Hart, JJ, RM Welch, WA Norvell, LA Sullivan, and LV Kochian. 1998. Characterization of cadmium binding, uptake, and translocation in intact seedlings of bread and durum wheat cultivars. *Plant Physiology* 116: 1413-1420.
- Hammer, D, A Kayser, and C Keller. 2003. Phytoextraction of Cd and Zn with *Salix viminalis* in field studies. *Soil Use and Management* 19: 187-192.
- Hilbert, JL, T Dubois, and J Vasseur. 1992. Detection of embryogenesis-related proteins during somatic embryo formation in *Cichorium*. *Plant Physiology and Biochemistry* 30: 733-741.
- Horsch, RB, JE Fry, NL Hoffman, D Eichholtz, SG Rogers, and RT Fraley. 1985. A simple and general method for transferring genes into plants. *Science* 227: 1229-1231.
- Ishizaki, K, S Chiyoda, KT Yamato, and T Kohchi. 2008. Agrobacterium-mediated

- transformation of the haploid liverwort *Marchantia polymorpha* L., an emerging model for plant biology. *Plant and Cell Physiology* 49: 1084-1091.
- Ito, M. 1962. Studies on the differentiation of fern gametophytes I. Regeneration of single cells isolated from cordate gametophytes of *Pteris vittata*. *Botanical Magazine Tokyo* 75: 19-27.
- Kadota, A and M Wada. 1989. Enzymatic isolation of protoplasts from fern protonemal cells stainable with fluorescent brightener. *Plant and Cell Physiology* 30: 1107-1113.
- Kato, Y. 1964. Physiological and morphogenetic studies of fern gametophytes by aseptic culture 3. *Cytologia* 29: 79-85.
- Kato, Y. 1967. Physiological and morphogenetic studies of fern gametophytes and sporophytes in aseptic culture. *Planta* 77: 127-134.
- Kato, Y. 1969. Physiological and morphogenetic studies of fern gametophytes and sporophytes in aseptic culture. *Phytomorphology* 19: 114-121.
- Kato, Y. 1970. Physiological and morphogenetic studies of fern gametophytes and sporophytes in aseptic culture. *Botanical Gazette* 131: 205-210.
- Kasprzak, KS. 1995. Possible role of oxidative damage in metal-induced carcinogenesis. *Cancer Investigation* 13 (4): 411-430.
- Kawakami, SM, M Ito, and S Kawakami. 1995. Apogamous sporophyte formation in a fern *Pteris multifida* and its characteristics. *Journal of Plant Research* 108: 181-184.

- Kaya, A and Y Yukselen. 2005. Zeta potential of soils with surfactants and its relevance to electrokinetic remediation. *Journal of Hazardous Materials B120*: 119-126.
- Kaźmierczak, A. 2003. Induction of cell division and cell expansion at the beginning of gibberellins A₃-induced precocious antheridia formation in *Anemia phyllitidis* gametophytes. *Plant Science* 5: 933-939.
- Kaźmierczak, A. 2007. Ethylene is a modulator of gibberellic acid-induced antheridiogenesis in *Anemia phyllitidis* gametophytes. *Biologia Plantarum* 51: 683-689.
- Kertész, S, Z Kerényi, Z Mérai, I Bartos, T Pálffy, E Barta, and D Silhavy. 2006. Both introns and long 3'-UTRS operate as *cis*-acting elements to trigger nonsense-mediated decay in plants. *Nucleic Acids Research* 34: 6147-6157.
- King, RF, A Royle, PD Putwain, and NM Dickinson. Changing contaminant mobility in a dredged canal sediment during a three-year phytoremediation trial. *Environmental Pollution* 143(2): 318-326.
- Kneer, R, and MH Zenk. 1992. Phytochelatins protect plant enzymes from heavy-metal poisoning. *Phytochemistry* 31 (8): 2663-2667.
- Koop, HU, K Steinmüller, H Wagner, C Rößler, C Eibl, and Lydia Sacher. 1996. Integration of foreign sequences into the tobacco plastome via polyethylene glycol-mediated protoplast transformation. *Planta* 199: 193-201.

- Krämer, U, IJ Pickering, RC Prince, I Raskin, and DE Salt. 2000. Subcellular localization and speciation of nickel in hyperaccumulator and non-accumulator *Thalasspi* species. *Plant Physiology* 122: 1343-1353.
- Kshirsagar, MK and AR Mehta. 1978. In vitro studies in ferns: growth and differentiation in rhizome callus of *Pteris vittata*. *Phytomorphology* 28: 50-58.
- Kwa, SH, YC Wee, and CS Loh. 1991. Production of aposporous gametophytes and calli from *Pteris vittata* L. pinnae strips cultured *in vitro*. *Plant Cell Reports* 10: 392-393.
- Lal, M and A Narang. 1985. Ultrastructural and histochemical studies of transfer cells in the callus and apogamous sporophytes of *Physcomitrium coorgense* Broth. *New Phytologist* 100: 225-231.
- Larkin, MA, G Blackshields, NP Brown, R Chenna, PA McGettigan, H McWilliam, F Valentin, IM Wallace, A Wilm, R Lopez, JD Thompson, TJ Gibson, and DG Higgins. 2007. Clustal W and clustal X version 2.0. *Bioinformatics* 23: 2947-2948.
- Lasat, MM. 2002. Phytoextraction of toxic metals: a review of biological mechanisms. *Journal of Environmental Quality* 31:109-120.
- Le Hir, H, E Izaurralde, LE Maquat and MJ Moore. 2000. The spliceosome deposits multiple proteins 20-24 nucleotides upstream of mRNA exon-exon junctions. *The EMBO Journal* 19: 6860-6869.

- Le Hir, H, D Gatfield, E Izaurralde, and MJ Moore. 2001. The exon-exon junction complex provides a binding platform for factors involved in mRNA export and nonsense-mediated mRNA decay. *The EMBO Journal* 20: 4987-4997.
- Lee, YW, CB Klein, B Kargacin, K Salnikow, J Kitahara, K Dowjat, A Zhitkovich, NT Christie, and M Costa. 1995. Carcinogenic nickel silences gene-expression by chromatin condensation and DNA methylation – A new model for epigenetic carcinogens. *Molecular and Cellular Biology* 15 (5): 2547-2557.
- Lewandowski, I, U Schmidt, M Londo, and A Faaij. 2006. The economic value of the phytoremediation function – assessed by the example of cadmium remediation by willow (*Salix* spp). *Agricultural Systems* 89: 68-89.
- Luo, M and R Reed. 1999. Splicing is required for rapid and efficient mRNA export in metazoans. *Proceedings of the National Academy of Sciences* 96: 14937-14942.
- Ma, LQ, KM Komar, C Tu, W Zhang, Y Cai, and ED Kenelley. 2001. A fern that hyperaccumulates arsenic. *Nature* 409: 579.
- Maeda, M and M Ito. 1981. Isolation of protoplasts from fern prothalli and their regeneration to gametophytes. *Botanical Magazine Tokyo* 94: 35-40.
- Maillet, C, RK Gupta, MG Schell, RG Brewton, CL Murphy, JS Wall, and BC Mullin. 2001. Enhanced capture of small histidine-containing polypeptides on membranes in the presence of ZnCl₂. *Biotechniques* 30: 1224–1228.
- Malik, K, K Wu, XQ Li, T Martin-Heller, M Hu, E Foster, L Tian, C Wang, K Ward, M Jordan, D Brown, S Gleddie, D Simmonds, S Zheng, J Simmonds, and B Miki.

2002. A constitutive gene expression system derived from the tCUP crptic promoter elements. *Theoretical Applied Genetics* 105: 505-514.
- Marklund, U, M Byström, K Gedda, Å Larefalk, K Juneblad, S Nyström, AJ Ekstrand. 2002. Intron-mediated expression of the human neuropeptide Y Y1 receptor. *Molecular and Cellular Endocrinology* 188: 85-97.
- Matsumoto, K, KM Wassarman, and AP Wolffe. 1998. Nuclear history of a pre-mRNA determines the translational activity of cytoplasmic mRNA. *The EMBO Journal* 17: 2107-2121.
- Mazarei, M, H Al-Ahmad, MR Rudis, and CN Stewart, Jr. 2008a. Protoplast isolation and transient gene expression in switchgrass, *Panicum virgatum* L. *Biotechnology Journal* 3: 354-359.
- Mazarei, M, I Teplova, MR Hajimorad, and CN Stewart. 2008b. Pathogen phytosensing: plants to report plant pathogens. *Sensors* 8: 2628-2641.
- Mejare, M., and Bulow, L. 2001. Metal-binding proteins and peptides in bioremediation and phytoremediation of heavy metals. *Trends in Biotechnology*. 19: 67–73.
- Mentewab, A, B Nelson, B Mullin, Z-M Cheng and CN Stewart, Jr. 2005. Metallothistins for phytoremediation. Twenty-Second Annual Missouri Symposium 'Genomics and Beyond: Frontiers in Plant Biology'. April 27-30, 2005, Columbia, Missouri.
- Moeller, L and K Wang. 2008. Engineering with precision: tools for the new generation of transgenic crops. *Bioscience* 58: 391-401.
- Murashige, T and F Skoog. 1962. A revised medium for rapid growth and bio assays with

- tobacco tissue cultures. *Physiologia Plantarum* 15: 473-497.
- Murphy, A, JM Zhou, PB Goldsbrough, and L Taiz. 1997. Purification and immunological identification of metallothioneins 1 and 2 from *Arabidopsis thaliana*. *Plant Physiology* 113 (4): 1293-1301.
- Muthukumar, B, B Yakubov, and DE Salt. 2007. Transcriptional activation and localization of expression of *Brassica juncea* putative metal transport protein BjMTPI. *BMC Plant Biology* 7: 32.
- Namasivayam, P, J Skepper, and D Hanke. 2006. Identification of a potential structural marker for embryogenic competency in the *Brassica napus* spp. *oleifera* embryogenic tissue. *Plant Cell Reports* 25: 887-895.
- Ovečka, M and M Bobák. 1999. Structural diversity of *Papaver somniferum* L. cell surfaces *in vitro* depending on particular steps of plant regeneration and morphogenetic program. *Acta Physiologiae Plantarum* 21: 117-126.
- Palta, HK and PN Mehra. 1983. *In vitro* induction of polyhaploid and octoploid *Pteris vittata* L. and their meiosis. *Caryologia* 36: 325-332.
- Park, CH, M Keyhan, and M Matin. 1999. Purification and characterization of chromium reductase in *Pseudomonas putida*. Abstract from General Meeting of the American Society of Microbiology 99: 536.
- Patel, M, AJ Siegel, and JO Berry. 2006. Untranslated regions of *FbRbcS1* mRNA mediate bundle sheath cell-specific gene expression in leaves of a C₄ plant. *The Journal of Biological Chemistry* 281: 25485-25491.

- Pawlowski, K, P Twigg, S Dobritsa, CH Guan, and B Mullin. 1997. A nodule-specific gene family from *Alnus glutinosa* encodes glycine- and histidine-rich proteins expressed in the early stages of actinorhizal nodule development. *Molecular Plant-Microbe Interactions* 10: 656–664.
- Perica, MC, F Gillet, A Jacquin-Dubreuil, M Krsnik-Rasol, and S Jelaska. 1998. Nicotine content in transformed haploid and dihaploid tissues of tobacco (*Nicotiana tabacum* L.). *Phyton-annales Rei Botanicae* 37: 229-239.
- Persans, MW, XG Yan, JMML Patnoe, U Krämer, DE Salt. 1999. Molecular dissection of the role of histidine in nickel hyperaccumulation in *Thlaspi goesingense*. *Plant Physiology* 121 (4): 1117-1126.
- Popielarska-Konieczna, M, M Kozieradzka-Kiszkurno, J Świerczyńska, G Góralski, H Ślesak, and J Bohdanowicz. 2008. Ultrastructure and histochemical analysis of extracellular matrix surface network in kiwifruit endosperm-derived callus culture. *Plant Cell Reports* 27: 1137-1145.
- Prada, C, V Moreno, and JM Gabriel y Galán. 2008. Gametophyte development, sex expression and antheridiogen system in *Pteris incomplete* Cav. (Pteridaceae). *American Fern Journal* 98: 14-25.
- Qu, GZ, GF Liu, YC Wang, J Jiang, and MH Wang. 2007. Efficient tissue culture and *Agrobacterium*-mediated transformation of haploid poplar derived from anthers. *Russian Journal of Plant Physiology* 54: 559-563.
- Raghavan, V. 1989. Control of differentiation of sex organs on gametophytes. In: PW

- Barlow, D Bray, PB Green, and JMW Slack, eds. *Developmental Biology of Fern Gametophytes*. Cambridge, Great Britain: Cambridge University Press 199-220.
- Rausser, WE. 1995. Phytochelatins and related peptides – structure, biosynthesis, and function. *Plant Physiology* 109 (4): 1141-1149.
- Rausser, WE. 1999. Structure and function of metal chelators produced by plants - The case for organic acids, amino acids, phytin, and metallothioneins. *Cell Biochemistry and Biophysiology* 31: 19–48.
- Rutherford, G, M Tanurdzic, M Hasebe, and JA Banks. 2004. A systemic gene silencing method suitable for high throughput, reverse genetic analyses of gene function in fern gametophytes. *BMC Plant Biology* 4: 6.
- Redford, K, MD Berliner, JE Gates, RW Fisher, and BF Matthews. 1987. Protoplast induction from sporophyte tissues of the heterosporous fern *Azolla*. *Plant Cell, Tissue and Organ Culture* 10: 187-196.
- Sandal, NN, K Bojsen, and KA Marcker. 1987. A small family of nodule specific genes from soybean. *Nucleic Acids Research*. 15: 1507-1519.
- Schallau, A, I Kakhovskaya, A Tewes, A Czihal, J Tiedemann, M Mohr, I Grosse, R Manteuffel, and H Bäumlein. 2008. Phylogenetic footprints in fern spore- and seed-specific gene promoters. *The Plant Journal* 53: 414-424.
- Schenk, PM, T Remans, L Sagi, AR Elliott, RG Dietzgen, R Swennen, PR Ebert, CPL Grof, and JM Manners. 2001. Promoters for pregenomic RNA of banana streak badnavirus are active for transgene expression in monocot and dicot plants. *Plant*

Molecular Biology 47: 399-412.

- Schwartz, AM, TV Komarova, MV Skulachev, AS Zvereva, YL Dorokhov, JG Atabekov. 2006. Stability of plant mRNAs depends on the length of the 3'-untranslated region. *Biochemistry (Moscow)* 71: 1377-1384.
- Sheffield, E, S Laird, and PR Bell. 1983. Ultrastructural aspects of sporogenesis in the apogamous fern *Dryopteris borreri*. *Journal of Cell Science* 63: 125-134.
- Shen, H and YT Wang. 1995. Modeling simultaneous hexavalent chromium reduction and phenol degradation by a defined coculture of bacteria. *Biotechnology and Bioengineering* 48: 606-613.
- Sivamani, E and R Qu. 2006. Expression enhancement of a rice polyubiquitin gene promoter. *Plant Molecular Biology* 60: 225-239.
- Sondahl, MR, JL Salisbury, and WR Sharp. 1979. SEM characterization of embryogenic tissue and flobular embryos during high frequency somatic embryogenesis in coffee callus cells. *Zeitschrift Fur Pflanzenphysiologie* 94: 185-187.
- Sugai, M. 1968. The changes of respiratory quotient during the early development in fern gametophytes. *Embryologia* 10: 164-172.
- Trotta, A, M Mantovani, A Fusconi, and C Gallo. 2007. In vitro culture of *Pteris vittata*, an arsenic hyperaccumulating fern, for screening and propagating strains useful for phytoremediation. *Caryologia* 60: 160-164.
- Virkutyte, J, M Sillanpää, and P Latostenmaa. 2002. Electrokinetic soil remediation – critical overview. *The Science of the Total Environment* 289: 97-121.

- Waalkes, MP, TP Coogan, and RA Barter. 1992. Toxicological principles of metal carcinogenesis with special emphasis on cadmium. *Critical Reviews in Toxicology* 22 (3-4): 175-201.
- Whittier, DP. 2003. Rapid gametophyte maturation in *Ophioglossum crotalophoroides*. *American Fern Journal* 93: 137-145.
- Yang, X, H Chen, W Xu, Z He, and M Ma. 2008. Hyperaccumulation of arsenic by callus, sporophytes and gametophytes of *Pteris vittata* cultured *in vitro*. *Plant Cell Reports* 26: 1889-1897.
- Zhao, FJ, SJ Dunham, and SP McGrath. 2002. Arsenic hyperaccumulation by different fern species. *New Phytologist* 156: 27-31.
- Zheng, YQ, WZ Xu, ZY He, and M Ma. 2008. Plant regeneration of the arsenic hyperaccumulator *Pteris vittata* L. from spores and identification of its tolerance and accumulation of arsenic and copper. *Acta Physiologiae Lantarum* 30: 249-255.
- Zhou, L, ZT Lai, MK Lu, XG Gong, and Y Xie. 2008. Expression and hydroxylamine cleavage of Thymosin alpha 1 concatemer. *Journal of Biomedicine and Biotechnology* DOI: 10.1155/2008/736060.

Vita

Blake Lee Joyce was born in Atlanta, GA on March 20, 1984. He was raised in Marietta, GA where he attended elementary school, middle school, and graduated from Wheeler High School in 2002. From there he went to the University of Georgia in Athens, GA and received a B.S. in Biology and another B.S. in Ecology in 2006. While working for Dr. Wayne Parrott, he met Dr. Neal Stewart and started work as a graduate research assistant in January 2007. He received his Master of Science degree in Plant Sciences with a minor in Statistics from the University of Tennessee, Knoxville in December 2008.